

## Excitation of particle-vibration multiplets in the $A = 110$ region by two-neutron stripping reactions\*

R. E. Anderson and J. J. Kraushaar

*Nuclear Physics Laboratory, Department of Physics and Astrophysics, University of Colorado,  
Boulder, Colorado 80309*

I. C. Oelrich, R. M. DelVecchio,<sup>†</sup> and R. A. Naumann

*Joseph Henry Laboratories, Princeton University, Princeton, New Jersey 08540*

E. R. Flynn and C. E. Moss

*Los Alamos Scientific Laboratory, Los Alamos, New Mexico 87545*

(Received 9 August 1976)

The  $^{103}\text{Rh}$ ,  $^{106,108}\text{Pd}$ , and  $^{107,109}\text{Ag}(t,p)$  reactions have been studied at a bombarding energy of 17 MeV. Excitation energies and enhancement factors were obtained for a number of levels up to about 2.5 MeV excitation in the residual nuclei. The  $L = 0$  transitions observed indicate that these nuclei are of a transitional character, though more closely resembling pairing rotational than pairing vibrational nuclei. The low-lying negative parity levels in the Ag nuclei appear to be well described as a  $(2p_{1/2})$  proton weakly coupled to the appropriate core state in the even Pd cores.  $^{105}\text{Rh}$  appears to display similar weak coupling characteristics. However, the higher-lying levels such as the  $3^-$  based states are severely mixed with single particle levels and perhaps with other elementary modes of excitation as well.

<p style="margin: 0;">NUCLEAR REACTIONS <math>^{103}\text{Rh}</math>, <math>^{106,108}\text{Pd}</math>, <math>^{107,109}\text{Ag}(t,p)</math>, <math>E(t) = 17.0</math> MeV, magnetic spectrograph, enriched targets; measured <math>\sigma(\theta, E_p)</math>, excitation energies, DWBA analysis; <math>^{105}\text{Rh}</math>, <math>^{108,110}\text{Pd}</math>, <math>^{109,111}\text{Ag}</math> deduced <math>L</math>, <math>J</math>, <math>\pi</math>, enhancement factors; weak coupling model.</p>
---

### I. INTRODUCTION

The idea of describing the states of an odd- $A$  nucleus in terms of a valence nucleon weakly coupled to the even-even core is not new.<sup>1,2</sup> There are, however, a rather limited number of nuclei that demonstrate clearly the features of the simple form of this model; the stable isotopes of silver,  $^{107}\text{Ag}$  and  $^{109}\text{Ag}$ , being two of the better examples. These nuclei are particularly favorable cases for the study of the weak coupling model since their ground states have a spin and parity of  $\frac{1}{2}^-$ . This means that the core coupled states will either be singlets, for  $0^+$  core states, or doublets for the other possibilities. The small number of members of a particular core multiplet minimizes the number of states in the multiplet which may mix with nearby single-particle states that have the same spin and parity and greatly facilitates the identification of the core multiplets.

The investigation of the weak coupling model has in the past been accomplished primarily by inelastic proton scattering and Coulomb excitation. More recently, however, the  $(p,t)$  and  $(t,p)$  reactions have proven extremely useful in extending the investigations to higher-lying states and to nuclei that are not stable. For example, recent studies with the  $(p,t)$  reaction have brought out quite

clearly the weak coupling features of  $^{107}\text{Ag}$ ,<sup>3,4</sup>  $^{105}\text{Ag}$ ,<sup>4</sup> and  $^{101}\text{Rh}$ .<sup>5</sup>

In order to further investigate the applicability of the weak coupling model to nuclei in the region of silver, the  $(t,p)$  reaction on  $^{103}\text{Rh}$ ,  $^{107}\text{Ag}$ , and  $^{109}\text{Ag}$  was studied. All three of these target nuclei have a ground state spin and parity of  $\frac{1}{2}^-$ . In addition, the  $^{106,108}\text{Pd}(t,p)^{108,110}\text{Pd}$  reactions were also studied in order to provide information on the phonons of the Pd cores for  $^{109}\text{Ag}$  and  $^{111}\text{Ag}$ .

In applying the simple harmonic weak coupling model to the  $(t,p)$  reaction, one assumes that the odd nucleon in the ground state of the odd- $A$  nucleus is simply a spectator during the transfer of two neutrons. For the even core, the  $(t,p)$  reaction is expected to populate primarily the pairing collective states of the residual nucleus, and the transitions observed in the neighboring odd- $A$  nucleus should be simply related to the corresponding core transitions. Specifically, the  $(t,p)$  transition should have the same summed strength to the various members of the particle-vibration multiplet as to the corresponding core state. Other predictions of the harmonic weak coupling model are that the excitation energy of the core state should be equal to the energy centroid of the multiplet, and that the  $(t,p)$  strength should be shared between the two levels of a multiplet in the

ratio of  $(2J_1 + 1)/(2J_2 + 1)$  where  $J_1$  and  $J_2$  are the spins of the levels involved. In the absence of a particle-core interaction the members of the multiplet are degenerate. Deviations from this simple behavior are to be expected and come about from such processes as mixing between the multiplets as well as mixing of the wave functions of the core coupled states with states of a different character—for example, single-particle states. The particle-vibrational model has been expanded theoretically to include such mixing,<sup>6,7</sup> and the overall concept has been shown to fit admirably into the concept of fundamental excitations of the nucleus.<sup>8</sup>

## II. EXPERIMENTAL PROCEDURE

The experiments were performed using a beam of 17 MeV tritons from the Los Alamos Scientific Laboratory FN tandem Van de Graaff accelerator. The targets, prepared by vacuum evaporation of metallic samples of Rh, Pd, and Ag onto carbon backings of about  $20 \mu\text{g}/\text{cm}^2$  areal density, had isotopic enrichments of 96% for  $^{106}\text{Pd}$  and 98% for  $^{108}\text{Pd}$ . The  $^{107}\text{Ag}$  and  $^{109}\text{Ag}$  enrichments were greater than 98%. As discussed later, thicknesses of the  $^{103}\text{Rh}$ ,  $^{106}\text{Pd}$ ,  $^{108}\text{Pd}$ ,  $^{107}\text{Ag}$ , and  $^{109}\text{Ag}$  targets were determined to be 160, 27, 84, 129, and  $92 \mu\text{g}/\text{cm}^2$ , respectively.

The outgoing protons were momentum analyzed in a Q3D type II magnetic spectrometer<sup>9</sup> operated at a solid angle of  $14.3 \text{ msr}$ . A helical-cathode position sensitive proportional counter<sup>10</sup> with an active length of about 100 cm was used in the focal plane of the spectrometer. Particle identification was achieved by combining the  $dE/dx$  information from the anode signal of the detector with the energy signal obtained from a plastic scintillator placed behind the proportional counter.

Typical proton spectra for the  $^{103}\text{Rh}$  and  $^{107,109}\text{Ag}(t,p)$  reactions are shown in Fig. 1. The other spectra are not shown but have similar peak widths and background rejection. The energy resolution varied somewhat with the target and with the position along the detector, but was in the range of 10 to 15 keV [full width at half maximum (FWHM)] for the lower-lying states. The peak shown at about 805 keV in the  $^{109}\text{Ag}$  spectrum is due to the  $^{109}\text{Ag}(t,p)^{111}\text{Ag}$  reaction to the ground state of  $^{111}\text{Ag}$ . This comes about because of the presence of a 1%  $^{109}\text{Ag}$  contaminant in the  $^{107}\text{Ag}$  target. A peak at a similar energy occurs in the  $^{108}\text{Pd}$  spectrum due to  $^{108}\text{Pd}$  in the  $^{106}\text{Pd}$  target. Centroids and peak areas were determined by fitting an empirically determined line shape to the various peaks using the code AUTOFIT.<sup>11</sup> Both the target thicknesses and the absolute normaliza-

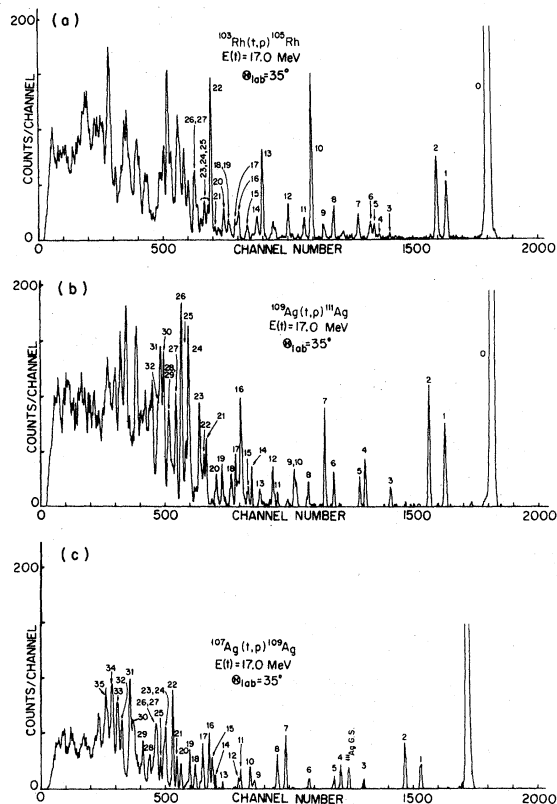


FIG. 1. (a) A typical spectrum observed in the  $^{103}\text{Rh}(t,p)^{105}\text{Rh}$  reaction. The states are numbered according to the identifications made in Table I. (b) A typical spectrum observed in the  $^{109}\text{Ag}(t,p)^{111}\text{Ag}$  reaction. The states are numbered according to the identifications made in Table V. (c) A typical spectrum observed in the  $^{107}\text{Ag}(t,p)^{109}\text{Ag}$  reaction. The states are numbered according to the identifications made in Table III.

tions of the data were determined by observing the elastically scattered tritons with a silicon surface barrier monitor detector positioned at  $30^\circ$  in the scattering chamber. The elastic cross sections were obtained from optical model predictions using parameters described below. Absolute cross sections for the  $(t,p)$  reactions were then based on the known solid angle of the spectrometer, the measured target thicknesses, and the integrated charge in the Faraday cup. Although absolute cross sections have uncertainties of about 20%, the use of constant optical potentials over such a limited mass range means that the relative normalizations among the five residual nuclei are determined to  $\pm 10\%$ . The angular distributions are shown in Figs. 2–6 and the error bars shown indicate only the statistical uncertainties of the individual data points.

The energies of the various states were determined in several ways. For all of the nuclei ex-

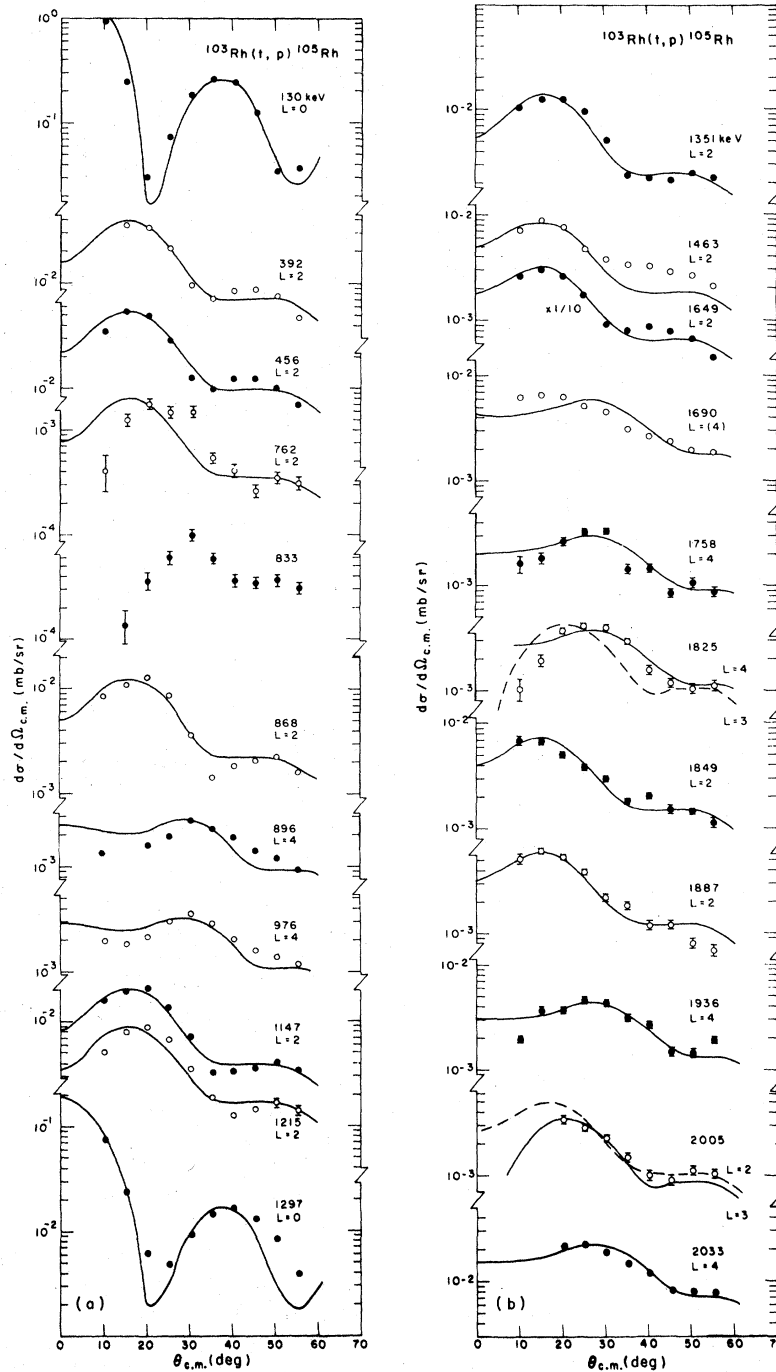


FIG. 2. (a) Angular distributions for states observed in  $^{105}\text{Rh}$ . The solid and dashed curves are the results of DWBA calculations described in the text.

cept  $^{105}\text{Rh}$  a number of states whose energies have been well determined were used for calibration purposes. Using a least squares procedure a second degree polynomial of proton momentum vs channel number was obtained and the energies of

the unknown states were generated from this. In Tables I to V the underlined energies were the ones assumed for calibration purposes. For  $^{105}\text{Rh}$ ,  $^{111}\text{Ag}$ , and  $^{110}\text{Pd}$  an external calibration was also obtained. Keeping the magnetic fields in the

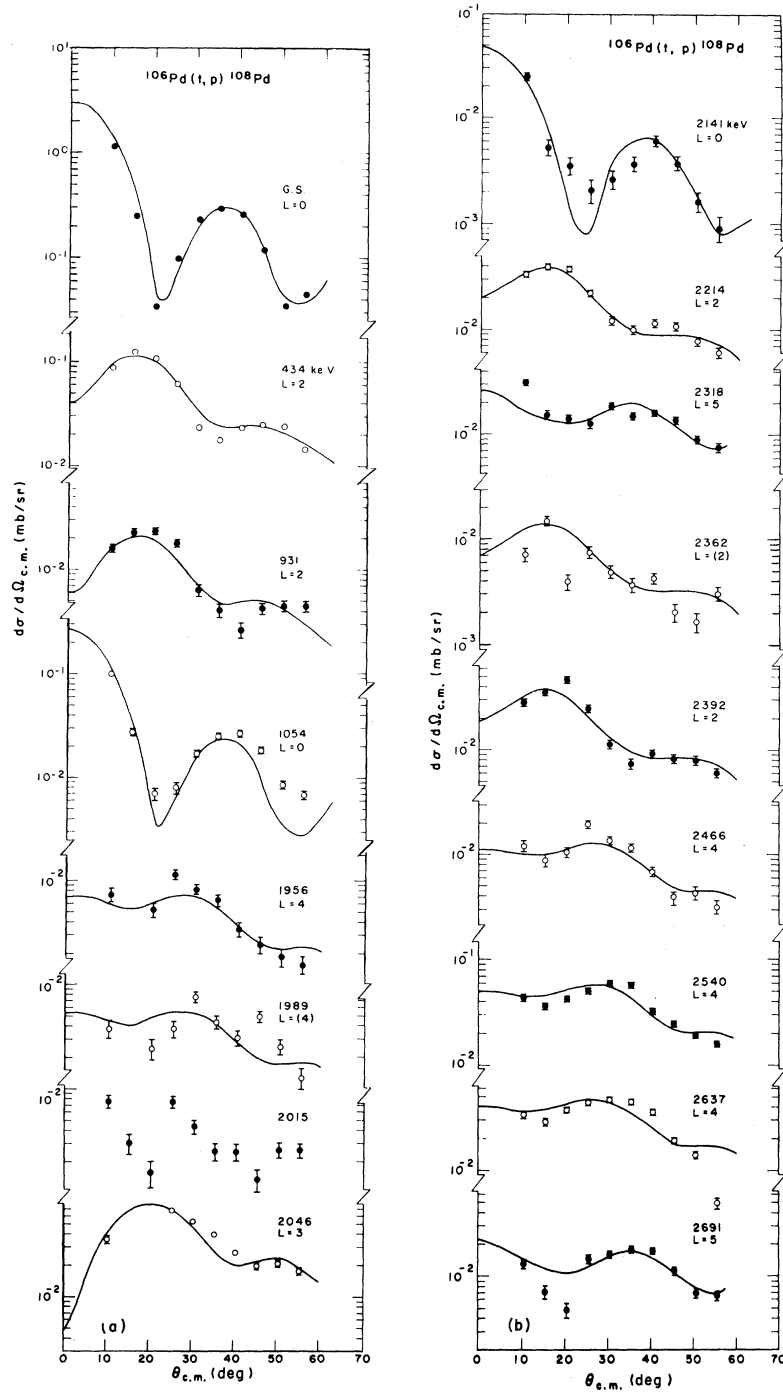


FIG. 3. (a), (b) Angular distributions for states observed in  $^{108}\text{Pd}$ . The solid and dashed curves are the results of DWBA calculations described in the text.

spectrometer fixed, data were taken for these nuclei and also the  $^{59}\text{Co}(t, p)$  reaction. Using information recently obtained<sup>12</sup> on the level energies of  $^{61}\text{Co}$  from the  $^{64}\text{Ni}(p, \alpha)$  reaction, the energies for the states in the above three targets were ob-

tained. A third procedure was also used for  $^{105}\text{Rh}$  since data were taken for  $^{109}\text{Ag}$  using the same spectrometer settings. This permitted the strong, well-defined states in  $^{109}\text{Ag}$  to be used for calibration purposes to obtain the energies for levels in

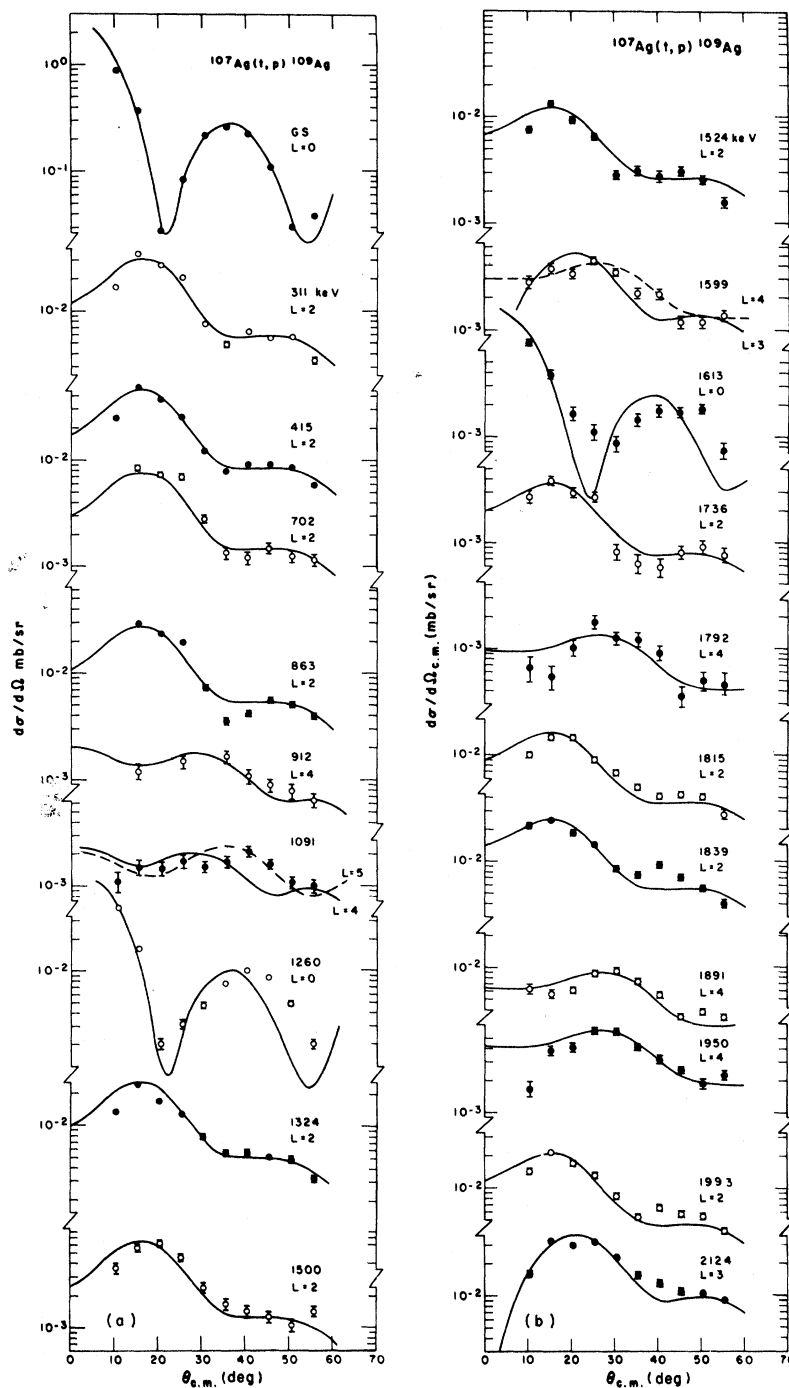


FIG. 4. (a), (b) Angular distributions for states observed in  $^{109}\text{Ag}$ . The solid and dashed curves are the results of DWBA calculations described in the text.

$^{105}\text{Rh}$ . In cases where the several procedures could be compared, the results were quite consistent. The uncertainties in the listed energies range from about 2 keV for the low-lying states to about 10 keV at the upper end of the spectra.

### III. DISTORTED WAVE BORN APPROXIMATION ANALYSIS

The experimental angular distributions are shown in Figs. 2 through 6. The solid lines shown are the results of distorted wave calculations per-

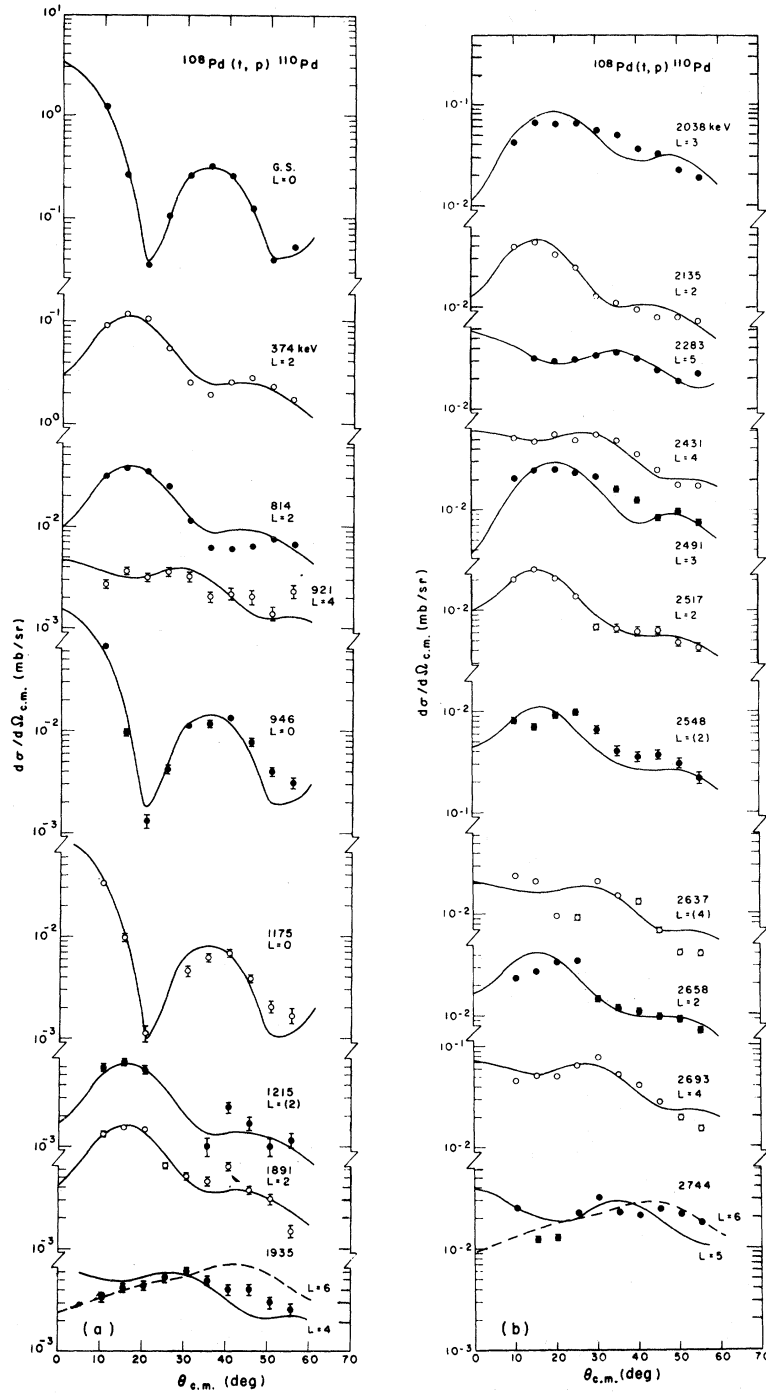


FIG. 5. (a), (b) Angular distributions for states observed in  $^{110}\text{Pd}$ . The solid and dashed lines are the results of DWBA calculations described in the text.

formed with the code DWUCK<sup>13</sup> which generates the two-nucleon form factor using the method of Bayman and Kallio.<sup>14</sup> The optical model and bound state parameters used are shown in Table VI. The proton parameters were taken from the work of

Perey<sup>15</sup> and the triton parameters from that of Flynn *et al.*<sup>16</sup> A  $(2d_{5/2})^2$  configuration was assumed for  $L=0, 2$ , and  $4$  transitions, a  $(1g_{7/2})^2$  configuration for  $L=6$ , a  $(1h_{11/2} \otimes 2d_{5/2})$  for  $L=3$  and  $5$ , and a  $(1h_{9/2} \otimes 1g_{7/2})$  configuration for  $L=1$ .

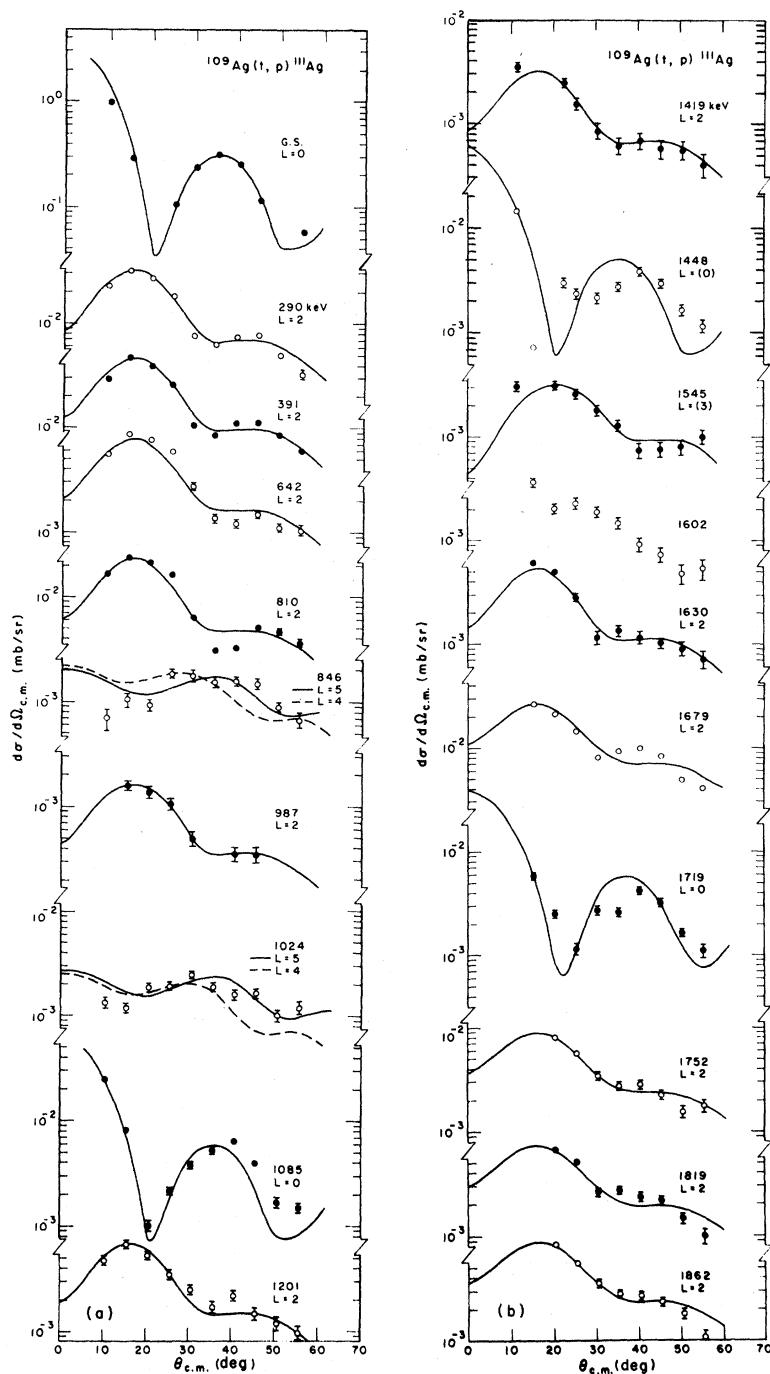


FIG. 6. (a), (b) Angular distributions for states observed in  $^{111}\text{Ag}$ . The solid and dashed lines are the results of DWBA calculations described in the text.

The differential cross section for the reaction  $A(t, p)B$  may be written

$$\left(\frac{d\sigma}{d\Omega}\right)_{\text{exp}} = N\epsilon \left(\frac{d\sigma}{d\Omega}\right)_{\text{DW}}, \quad (1)$$

where the normalization constant  $N$  is taken to be

218. The remaining quantity is the enhancement factor  $\epsilon$ , which is the factor necessary to yield equality between the right and left hand sides of Eq. (1). In the usual analysis assuming a single step reaction mechanism, the distorted wave Born approximation (DWBA) predicted shape for a tran-

TABLE I. Level structure of  $^{105}\text{Rh}$ . The excitation energies, enhancement factors, and spin-parity assignments for levels observed in  $^{105}\text{Rh}$  are shown together with the results of previous investigations. Spin assignments are placed in parentheses if either the  $L$  transfer is uncertain or if one of the two possible final state spins is suggested.

Level No.	Present results			Nuclear data sheets <sup>a</sup>			$^{105}\text{Ru}$ decay <sup>b</sup>			$^{86}\text{Zr}(^{12}\text{C}, p2m\gamma)^{105}\text{Rh}^c$		
	$E$ (keV)	$L$	Enhancement factor $\epsilon$	$E$ (keV)	$J^\pi$	$J^\pi$	$E$ (keV)	$J^\pi$	$J^\pi$	$E$ (keV)	$J^\pi$	$J^\pi$
0	0			0	$(\frac{1}{2})^+$	$(\frac{1}{2})^+$	0	$\frac{1}{2}^+$	$\frac{1}{2}^+$	0	$\frac{1}{2}^+$	$\frac{1}{2}^+$
0	<u>130</u>	0	2.27	129.7	$(\frac{1}{2})^-$	$(\frac{1}{2})^-$	129.61	$\frac{1}{2}^-$	$\frac{1}{2}^-$	130	$\frac{1}{2}^-$	$\frac{1}{2}^-$
1	<u>392</u>	2	0.10	149.2	$(\frac{3}{2})^-$	$(\frac{3}{2})^-$	149.10	$\frac{3}{2}^+$	$\frac{3}{2}^+$	149	$\frac{3}{2}^+$	$\frac{3}{2}^+$
2	<u>456</u>	2	0.131	392.6	$(\frac{3}{2})^-$	$(\frac{3}{2})^-$	392.44	$\frac{3}{2}^-$	$\frac{3}{2}^-$	392	$\frac{3}{2}^-$	$\frac{3}{2}^-$
				410 ?			455.75	$\frac{5}{2}^-$	$\frac{5}{2}^-$	456	$\frac{5}{2}^-$	$\frac{5}{2}^-$
				455.9	$(\frac{5}{2})^-$	$(\frac{5}{2})^-$	469.37	$\frac{3}{2}^+$	$\frac{3}{2}^+$			
				469.4	$(\frac{5}{2})^+$	$(\frac{5}{2})^+$	499.26	$\frac{5}{2}^+$	$\frac{5}{2}^+$			
				499.2	$(\frac{5}{2})^+$	$(\frac{5}{2})^+$						
				524			638.66	$\frac{7}{2}^+$	$\frac{7}{2}^+$	603	$\frac{11}{2}^+$	$\frac{11}{2}^+$
				638.6	$(\frac{5}{2}, \frac{7}{2})^+$	$(\frac{5}{2}, \frac{7}{2})^+$	724.21	$\frac{5}{2}^+$	$\frac{5}{2}^+$			
				724.5	$(\frac{5}{2})^+$	$(\frac{5}{2})^+$	761.95	$\frac{3}{2}^-$	$(\frac{1}{2})^-$			
3	762	2	0.005	762.0	$(\frac{3}{2})^+$	$(\frac{3}{2})^+$	785.6	$(\frac{1}{2}, \frac{3}{2})^-$	$(\frac{1}{2}, \frac{3}{2})^-$	795	$\frac{13}{2}^+$	$\frac{13}{2}^+$
				785.9	$(\frac{3}{2})^-$	$(\frac{3}{2})^-$	808.1	$\frac{3}{2}^+$	$\frac{3}{2}^+$			
				808.1	$(\frac{3}{2})^+$	$(\frac{3}{2})^+$	817					
				817								
4	833			858	$(\frac{1}{2}, \frac{3}{2})^-$	$(\frac{1}{2}, \frac{3}{2})^-$	842.5					
5	868	2	0.029		$(\frac{5}{2})^-$	$(\frac{5}{2})^-$						
6	896	4	0.007	898	$(\frac{1}{2})^-$	$(\frac{1}{2})^-$	969.5	$\frac{3}{2}^+$	$\frac{3}{2}^+$	978	$\frac{9}{2}^-$	$\frac{9}{2}^-$
				924	$(\frac{1}{2}, \frac{3}{2})^-$	$(\frac{1}{2}, \frac{3}{2})^-$						
				969.5	$(\frac{5}{2})^+$	$(\frac{5}{2})^+$						
7	976	4	0.009	1016 ?	$(\frac{9}{2})^-$	$(\frac{9}{2})^-$						
				1062								
				1126								
8	1147	2	0.050	1190	$\frac{3}{2}, \frac{5}{2}^-$	$\frac{3}{2}, \frac{5}{2}^-$						
9	1215	2	0.021	1215.2	$\frac{3}{2}, \frac{5}{2}^-$	$\frac{3}{2}, \frac{5}{2}^-$						
				1269 ?								
10	1297	0	0.151	1321.3	$\frac{1}{2}^-$	$\frac{1}{2}^-$	1316.3					
							1321.26	$\frac{5}{2}^+$	$\frac{5}{2}^+$			

TABLE I (Continued)

Level No.	Present results		Enhancement factor $\epsilon$	$J^\pi$	Nuclear data sheets <sup>a</sup>		<sup>105</sup> Ru decay <sup>b</sup>		<sup>96</sup> Zr( <sup>12</sup> C, p2 $\alpha$ ) <sup>105</sup> Rh <sup>c</sup>	
	E (keV)	L			E (keV)	$J^\pi$	E (keV)	$J^\pi$	E (keV)	$J^\pi$
11	1351	2	0.033	$\frac{3}{2}^-, \frac{5}{2}^-$	1345.2 (1368)	$(\frac{3}{2}^-, \frac{5}{2}^+)$	1345.18	$(\frac{3}{2}^+)$		
					1377.1		1377.06	$\frac{3}{2}^+$		
					1393		1441.2			
12	1463	2	0.022	$\frac{3}{2}^-, \frac{5}{2}^-$	1442		1486.84	$(\frac{3}{2}^+)$		
					1486.6	$(\frac{5}{2}^-, \frac{7}{2}^-)$				
					1521				1535	$\frac{17}{2}^+$
					1543 ?					
					1577				1646	$\frac{13}{2}^-$
13	1649	2	0.008	$\frac{3}{2}^-, \frac{5}{2}^-$			1697.5			
14	1690	(4)	0.012	$(\frac{1}{2}^-, \frac{3}{2}^-)$						
15	1758	4	0.005	$\frac{7}{2}^-, \frac{9}{2}^-$			1720.3			
16	1825	(3, 4)		$(\frac{5}{2}^+, \frac{7}{2}^+, \frac{9}{2}^-)$			1762			$\frac{7}{2}^+$
17	1849	2	0.018	$\frac{3}{2}^-, \frac{5}{2}^-$			(1829)			
18	1887	2	0.015	$\frac{3}{2}^-, \frac{5}{2}^-$			1864			
19	1904	(2)		$(\frac{3}{2}^-, \frac{5}{2}^-)$			1913			$\frac{3}{2}^+, \frac{5}{2}^+$
20	1936	4	0.009	$\frac{7}{2}^-, \frac{9}{2}^-$			1957			
21	2005	2, 3		$\frac{3}{2}^-, \frac{5}{2}^+, \frac{7}{2}^+$						
22	2033	4	0.040	$\frac{7}{2}^-, \frac{9}{2}^-$						
23	2061	4	0.009	$\frac{7}{2}^-, \frac{9}{2}^-$						
24	2083	4	0.008	$\frac{7}{2}^-, \frac{9}{2}^-$						
25	2109	2	0.031	$\frac{3}{2}^-, \frac{5}{2}^-$						
26	2137	4	0.009	$\frac{7}{2}^-, \frac{9}{2}^-$						
27	2160	(2)	0.011	$(\frac{3}{2}^-, \frac{5}{2}^-)$						

<sup>a</sup> Reference 17.<sup>b</sup> References 18 and 20.<sup>c</sup> Reference 19.

TABLE II. Level structure of  $^{108}\text{Pd}$ . Since the target ground state is  $0^+$ , the final state spin and parity is given by  $J=L, \pi=(-1)^L$ .

Level No.	Present results			$^{108}\text{Pd}(n, n'\gamma)^a$		$^{108}\text{Pd}(p, p')^b$		$^{108}\text{Ag decay}^c$		Nuclear data sheets <sup>d</sup>		$^{108}\text{Ag}^m \text{ decay}^e$		$^{108}\text{Ag}^m \text{ decay}^f$	
	$E$ (keV)	$L$	$\epsilon$	$E$ (keV)	$J^\pi$	$E$ (keV)	$J^\pi$	$E$ (keV)	$J^\pi$	$E$ (keV)	$J^\pi$	$E$ (keV)	$J^\pi$	$E$ (keV)	$J^\pi$
0	0	0	2.37	g.s.	$0^+$	g.s.	$0^+$	g.s.	$0^+$	g.s.	$0^+$	g.s.	$0^+$	g.s.	$0^+$
1	434	2	0.30	433.9	$2^+$	430	$2^+$	433.9	$2^+$	433.95	$2^+$	434.00	$2^+$	434.0	$2^+$
2	931	2	0.044	931.2	$2^+$	930	$2^+$	930.9	$2^+$	931.2	$2^+$	930.4	$2^+$	931.0	$2^+$
3	1054	0	0.214	1048.1	$4^+$	1050	$4^+, 0^+$	1052.8	$0^+$	1048.32	$(4)^+$	1048.37	$(4)^+$	1048.3	$4^+$
				1052.6	$0^+$			1314.1		1052.80	$(0)^+$			1052.7	$0^+$
				1314.2	$(0)^+$			1314.1		1314.21	$(0)$				
				1335.2	$(3^+)$			1441.1	$2^+$	1335.6					
				1441.3	$(2^+)$	1420		1540.0	$(1^+, 2^+)$	1441.14				1440.9	$(1, 2)$
				1540.0	$(1^+, 2^+)$			1540.0		1539.9				1539.4	$(1, 2)$
4	1956	4	0.021	1770.9	$6^+$			1610		1771.32	$(6)^+$	1771.32	$6^+$	1771.2	$6^+$
5	1989	(4)	0.016												
6	2015														
7	2046	3	0.263	2046.6	$3^-$	2030	$3^-$			2046	$(3^-)$				
8	2141	(0)	0.050												
9	2214	2	0.102	2218.1											
				2282.5											
10	2318	5	0.060			2330									
11	2362	(2)	0.036												
12	2392	2	0.097												
13	2418														
14	2466	4	0.029	2477.6											
15	2540	4	0.133	2540.3		2530									
16	2578														
17	2637	4	0.112												
18	2691	(5)	0.056			2680									
19	2726	2	0.107	2720.0											
				2888.7		2850									
						2930									
						3140									

<sup>a</sup> Reference 27.<sup>b</sup> Reference 28.<sup>c</sup> Reference 23.<sup>d</sup> Reference 22.<sup>e</sup> Reference 25.<sup>f</sup> Reference 24.<sup>g</sup> Reference 26.

TABLE III. Level structure of  $^{103}\text{Ag}$ . See the caption for Table I for further explanation.

Level No.	Present results				Nuclear data sheets <sup>a</sup>		$(p, p')$ <sup>b</sup> $l$	$(^3\text{He}, d)$ <sup>c</sup>	
	$E$ (keV)	$L$	$\epsilon$	$J^\pi$	$E$ (keV)	$J^\pi$		$E$ (keV)	$l$
0	0	0	2.24	$\frac{1}{2}^-$	0	$\frac{1}{2}^-$	0	0	1
					88.0	$\frac{7}{2}^+$			
					132.8	$(\frac{9}{2})^+$		131	4
1	<u>311</u>	2	0.070	$(\frac{3}{2}^-)$	311.4	$\frac{3}{2}^-$	2	311	1
2	<u>415</u>	2	0.105	$(\frac{5}{2}^-)$	415.3	$\frac{5}{2}^-$	2		
3	<u>702</u>	2	0.018	$(\frac{3}{2}^-)$	701.9	$\frac{3}{2}^-$	2		
					724.4	$(\frac{3}{2})^+$		706	0
					735.3	$(\frac{5}{2})^+$		731	2
					839.8				
4	<u>863</u>	2	0.064	$(\frac{5}{2}^-)$	862.7	$\frac{5}{2}^-$	2		
					869.5	$(\frac{5}{2})^+$		866	2
					911.0			910	4
5	<u>912</u>	4	0.060	$(\frac{7}{2}^-)$	912.3				
6	<u>1091</u>	4, 5	0.075 if 4 0.100 if 5	$(\frac{9}{2}^-)$	1090.6 1099 ?		4		
								1200	(2, 4)
7	1260	0	0.085	$\frac{1}{2}^-$	1260		0	1255	(1)
8	<u>1324</u>	2	0.058	$\frac{3}{2}^-, \frac{5}{2}^-$	1324.2	$(\frac{3}{2}^-)$		1310	(1, 2, 4)
								1430	0
								1490	2
9	1500	2	0.015	$\frac{3}{2}^-, \frac{5}{2}^-$	1510		4		
10	1524	2	0.028	$\frac{3}{2}^-, \frac{5}{2}^-$					
11	1599	(3, 4)		$(\frac{5}{2}^+, \frac{7}{2}^+, \frac{9}{2}^-)$				1600	
12	1613	0	0.015	$\frac{1}{2}^-$	1610				
								1658	0
13	1736	2	0.08	$\frac{3}{2}^-, \frac{5}{2}^-$				1750 ?	
14	1792	4	0.003	$\frac{7}{2}^-, \frac{9}{2}^-$					
15	1815	2	0.038	$\frac{3}{2}^-, \frac{5}{2}^-$					
16	1839	2	0.058	$\frac{3}{2}^-, \frac{5}{2}^-$				1841	2
17	1891	4	0.019	$\frac{7}{2}^-, \frac{9}{2}^-$					
18	1950	4	0.012	$\frac{7}{2}^-, \frac{9}{2}^-$				1970	2
19	1993	2	0.050	$\frac{3}{2}^-, \frac{5}{2}^-$				2000 ?	
								2030 ?	
20	2062	4	0.014	$\frac{7}{2}^-, \frac{9}{2}^-$				2070 ?	
21	2093	2	0.042	$\frac{3}{2}^-, \frac{5}{2}^-$					
22	2124	3	0.102	$\frac{5}{2}^+, \frac{7}{2}^+$				2130	(2, 4)
23	2185	(4)	0.024	$(\frac{7}{2}^-, \frac{9}{2}^-)$	2150	$\frac{5}{2}^+, \frac{7}{2}^+$	3		
24	2199	(4)	0.013	$(\frac{7}{2}^-, \frac{9}{2}^-)$					
25	2222	(4)	0.012	$(\frac{7}{2}^-, \frac{9}{2}^-)$	2230	$\frac{5}{2}^+, \frac{7}{2}^+$	3	2220	(2, 4)
26	2256	5	0.035	$\frac{9}{2}^+, \frac{11}{2}^+$					
27	2267	3	0.068	$\frac{5}{2}^+, \frac{7}{2}^+$					
28	2314	(2)	0.045	$(\frac{3}{2}^-, \frac{5}{2}^-)$				2320	0

TABLE III (Continued)

Level No.	Present results				Nuclear data sheets <sup>a</sup>		$(p, p')$ <sup>b</sup> $l$	$(^3\text{He}, d)$ <sup>c</sup>	
	$E$ (keV)	$L$	$\epsilon$	$J^\pi$	$E$ (keV)	$J^\pi$		$E$ (keV)	$l$
29	2364	5	0.019	$\frac{9}{2}^+, \frac{11}{2}^+$			2400	(2, 5)	
30	2434	4	0.034	$\frac{7}{2}^-, \frac{9}{2}^-$					
31	2466	4	0.054	$\frac{7}{2}^-, \frac{9}{2}^-$			2470	0	
32	2537	5	0.040	$\frac{9}{2}^+, \frac{11}{2}^+$					
33	2569	(5)	0.067	$(\frac{9}{2}^+, \frac{11}{2}^+)$					
34	2614	(4)	0.062	$(\frac{7}{2}^-, \frac{9}{2}^-)$					
35	2659						3275	2	

<sup>a</sup> Reference 29.<sup>b</sup> Reference 30.<sup>c</sup> Reference 31.

sition of a particular  $L$  value is generally insensitive to the transfer configuration. Thus,  $\epsilon$  is a kinematically corrected factor which indicates deviations of the true two-nucleon overlap values from those assumed in the calculations (in this work the pure configurations listed above were assumed). Even if such complications as two step processes are present,  $\epsilon$  is still a convenient parametrization of the data since the two step processes should occur for both the odd- $A$  and even- $A$  targets with about the same probability. The enhancement factors obtained based on the above configurations are listed in Tables I to V. The theoretical cross sections were averaged over the in-plane acceptance angle of the spectrometer to yield the theoretical curves shown in Figs. 2 through 6.

#### IV. EXPERIMENTAL RESULTS

##### A. $^{105}\text{Rh}$

Table I and Fig. 2 show the results for  $^{105}\text{Rh}$ . In addition to the work included in the Nuclear Data Sheets,<sup>17</sup> three recent contributions have been made to the level structure information on  $^{105}\text{Rh}$ . Aras and Walters<sup>18</sup> studied the decay of  $^{105}\text{Ru}$  and have made the assignments shown in Table I while Grau *et al.*<sup>19</sup> observed the  $\gamma$  rays following the  $^{96}\text{Zr}(^{12}\text{C}, p2n\gamma)^{105}\text{Rh}$  reaction and Schneider *et al.*<sup>20</sup> have measured a series of  $\gamma$ -ray angular correlations following the decay of  $^{105}\text{Ru}$ .

The information from the  $(t, p)$  reaction tends to confirm previous assignments for the states at 130, 392, 456, and 762 keV. Since  $^{103}\text{Rh}$  has a nonzero ground state spin, only  $L=0$  transitions lead to states of unambiguous  $J^\pi$  in the residual nucleus while transitions of higher multipolarity

can populate states with  $J = L \pm \frac{1}{2}$ ,  $\pi = (-1)^L$  where  $\frac{1}{2}$  is the ground state spin of  $^{103}\text{Rh}$ . Since  $j = \frac{1}{2}$  for all the odd- $A$  targets, two final state spins are possible for each nonzero  $L$ . The lowest transition observed is an  $L=0$  transition to the  $\frac{1}{2}^-$  level at 130 keV. The ground state of  $^{105}\text{Rh}$  involves a different proton configuration than that found in the  $^{103}\text{Rh}$  ground state, and this transition was too weak to be observed indicating very little neutron admixture. As discussed later, the properties of the  $L=2$  transitions to the states at 392 and 456 keV are consistent with these states having the previously assigned spins and parities of  $\frac{3}{2}^-$  and  $\frac{5}{2}^-$ , respectively. The state at 762 keV is apparently the lower spin member of the  $2_2^+$  doublet, which would be consistent with the  $\frac{3}{2}^-$  assignment of Aras and Walters<sup>18</sup> but not the  $(\frac{3}{2})^+$  assignment of others.<sup>17</sup>

The 833 and 868 keV levels have apparently not been observed previously (although the 868 level could conceivably be the 858 keV level of Ref. 17, it is not likely), while the 896 keV level is most probably the 898 keV state seen in the  $(p, \alpha)$  and  $(^3\text{He}, d)$  reactions.<sup>21</sup> The  $L=4$  assignment from the  $(t, p)$  reaction would select just the  $\frac{7}{2}^-$  from the two possibilities from the  $(p, \alpha)$  studies.<sup>21</sup>

It is interesting that the  $L=4$  transition to the level at 976 keV agrees rather nicely with the  $\frac{9}{2}^-$  assignment made recently by Grau *et al.*<sup>19</sup> to a level they put at 978 keV. Of the higher-lying states, only the  $L=2$  transition to the 1215 keV state can, with any certainty, be associated with levels observed by others, but here there is no spin assignment to compare to the  $\frac{3}{2}^-$  or  $\frac{5}{2}^-$  assignments of the present study. The  $L=0$  assignment to the 1297 keV level makes this spin assignment a definite  $\frac{1}{2}^-$ .

TABLE IV. Level structure of  $^{110}\text{Pd}$ . See the caption for Table II for further explanation.

Level No.	Present results			Nuclear data sheets <sup>a</sup>	
	$E$ (keV)	$L$	$\epsilon$	$E$ (keV)	$J^\pi$
0	0	0	2.52	0	$0^+$
1	<u>374</u>	2	0.29	373.8	$2^+$
2	<u>814</u>	2	0.095	813.8	$2^+$
3	<u>921</u>	4	0.010	920.5	$4^+$
4	<u>946</u>	0	0.11	946.3	$0^+$
5	1175	0	0.068	1168	
6	1215	(2)	0.016	1212.4	$(2^+)$
				1309 ?	
				1397.8	
				1472	
				1574.1	
				1641 ?	
				1713	$(6^+)$
7	1891	(2)	0.04	1900.4	
8	1935	(4)	0.015	1933	$(6^+)$
9	<u>2038</u>	3	0.266	2038	$(3^-)$
10	2135	2	0.11	2135	$(1^-)$
				2193	$(3^-, 5^-)$
11	2283	5	0.13	2293	$(4^+)$
				2370	
12	2431	4	0.12	2446	$(3^-)$
				2447.1	
13	2491	3	0.089	2499	$(4^+)$
14	2517	2	0.065	2526 ?	
15	2548	(2)	0.029	2554	
16	2637	(4)	0.042		
17	2658	2	0.105	2673	
18	2693	4	0.14		
				2713	$(4^+)$
19	2744	(5, 6)			
20	2760			2778	$(3^-)$
				2791.1	
				2804.7	
				2888	
				2946	
				2983	
				3010	

<sup>a</sup> Reference 32.

#### B. $^{108}\text{Pd}$

Table II summarizes the data from the  $^{106}\text{Pd}$ - $(t, p)^{108}\text{Pd}$  reaction and Fig. 3 displays the angular distributions. The result of other investigations<sup>22-28</sup> are also included in Table II. The properties of the ground and first two excited states of  $^{108}\text{Pd}$  seem to be agreed upon by all observers. The resolution of the  $(t, p)$  experiment was not sufficient to separate the 1048 keV  $4^+$  state in the presence of the strong 1054 keV  $L=0$  transition. In fact neither the peak width nor the angular distribution of the state at 1054 keV were measurably changed by the presence of the 1048 keV state indicating a relatively weak population

of this level. The octupole state at 2046 keV appears as a strong  $L=3$  transition in the  $(t, p)$  data. The association with previously established levels seems uncertain for the next three states seen in the present studies at 2141, 2214, and 2318 keV. It is interesting that the  $0^+$  state at 1314 keV and the  $2^+$  state at 1441 keV were not seen, but this could be due to the fact that the  $^{106}\text{Pd}$  target was unfortunately quite thin and cross sections below a few  $\mu\text{b}$  were not observed.

#### C. $^{109}\text{Ag}$

As is shown in Table III, there is good agreement between the assignments made to the levels up through the 863 keV state from the compilation of Bertrand<sup>29</sup> and the inelastic proton scattering of Ford *et al.*<sup>30</sup> and  $L$  values determined from the  $(t, p)$  data shown in Fig. 4. In each case the  $\frac{3}{2}^-$  member of the doublets based on the  $2_1^+$  and  $2_2^+$  states lies below the  $\frac{5}{2}^-$  member. Although the  $(t, p)$  angular distributions are not definitive on the point, the states at 912 and 1091 keV are probably the  $\frac{7}{2}^-$  and  $\frac{9}{2}^-$  members of the  $4_1^+$  vibration multiplet with probably the  $\frac{7}{2}^-$  member again being the lowest-lying member at 912 keV.

The state at 1260 keV populated with an  $L$  transfer of 0 can be assigned  $J^\pi = \frac{1}{2}^-$ . Above 1324 keV little correspondence between the  $(t, p)$  data and the data of Refs. 29 and 31 can be drawn. The negative parity assignment for the 1839 keV level seen in the  $(t, p)$  reaction is inconsistent with that of Auble *et al.*<sup>31</sup> for their level at 1841 keV. In addition, the 2124 and 2267 keV members of the octupole multiplet appear at distinctly different excitation energies from those determined in Ref. 30.

#### D. $^{110}\text{Pd}$

The information on the level structure of  $^{110}\text{Pd}$  is listed in the Nuclear Data Sheets.<sup>32</sup> That information as well as a summary of the  $(t, p)$  data for  $^{110}\text{Pd}$  is listed in Table IV with the  $L$  values and enhancement factors obtained from the angular distributions shown in Fig. 5. A consistent picture is present at least up through the 946 keV state. The 1175 keV state seen in the present work is definitely a  $0^+$  state but it is not clear that it is to be associated with the 1168 keV level seen by others.<sup>32</sup> The state observed at 1935 keV appears to have an  $L$  transfer of 4 although 5 or 6 cannot be excluded. The latter would be consistent with the assignment of  $6^+$  made by Robinson *et al.*<sup>33</sup> in an inelastic proton scattering experiment. An  $L$  value of 3 appears most likely for the state at 2038 keV from the  $(t, p)$  angular distributions. It seems clear that this is the octupole state that is strongly excited both in the  $(t, p)$  and  $(p, p')$  reactions.

TABLE V. Level structure of  $^{111}\text{Ag}$ . See the caption for Table I for further explanation.

Level No.	$E$ (keV)	$L$	Present results		$^{111}\text{Pd}$ decay <sup>a</sup>		$^{111}\text{Pd}$ decay <sup>b</sup>	
			$\epsilon$	$J^\pi$	$E$ (keV)	$J^\pi$	$E$ (keV)	$J^\pi$
0	0	0	2.70	$\frac{1}{2}^-$	0	$\frac{1}{2}^-$	0	$\frac{1}{2}^-$
					59.9	$\frac{7}{2}^+$	59.8	$\frac{7}{2}^+$
					130.4	$(\frac{9}{2}^+)$	130.2	$(\frac{9}{2}^+)$
1	<u>290</u>	2	0.084	$(\frac{3}{2}^-)$	289.8	$(\frac{3}{2}^-)$	289.8	$(\frac{3}{2}^-)$
					376.7	$\frac{3}{2}^+, \frac{5}{2}^-$	376.7	$(\frac{3}{2}^+, \frac{5}{2}^-)$
2	<u>391</u>	2	0.118	$(\frac{5}{2}^-)$	391.3	$(\frac{5}{2}^-)$	391.2	$(\frac{5}{2}^-)$
					404.9	$\frac{1}{2}^+, \frac{3}{2}^+, \frac{5}{2}^-$	404.9	
					546.0	$\frac{5}{2}^+, \frac{7}{2}^+$	545.6	$(\frac{7}{2}^+, \frac{5}{2}^+)$
					568.8	$\frac{5}{2}^+, \frac{7}{2}^-$	568.7	$(\frac{5}{2}^+, \frac{7}{2}^-)$
					607.1	$\frac{5}{2}^+, \frac{7}{2}^+$	606.9	$(\frac{5}{2}^+, \frac{7}{2}^+)$
3	<u>642</u>	2	0.020	$(\frac{3}{2}^-)$	642.4	$\frac{3}{2}^-, \frac{5}{2}^-$		
					683.2	$\frac{7}{2}^-$	683.0	
					705.5	$\frac{7}{2}^+, \frac{9}{2}^+, \frac{11}{2}^+$	705.2	$(\frac{11}{2}^+, \frac{9}{2}^+)$
					710.5	$\frac{5}{2}^+, \frac{7}{2}^+$	710.3	$(\frac{5}{2}^+, \frac{7}{2}^+)$
4	810	2	0.060	$(\frac{5}{2}^-)$	809.0	$\frac{5}{2}^-$		
					824.5	$\frac{9}{2}^+, \frac{11}{2}^+$	824.4	$\frac{11}{2}^+, \frac{13}{2}^+$
5	<u>846</u>	(4, 5)	{ 0.0050 if 4 0.0065 if 5	$(\frac{7}{2}^-)$	846.0	$\frac{5}{2}^-, \frac{7}{2}^-$	845.6	$\frac{7}{2}^-, \frac{9}{2}^-$
					876.7	$\frac{7}{2}^+, \frac{9}{2}^+, \frac{11}{2}^+$	876.3	
							903.9	
					959	$\frac{9}{2}^+, \frac{11}{2}^+$	958.8	$(\frac{9}{2}^+)$
6	987	2	0.0042	$\frac{3}{2}^-, \frac{5}{2}^-$	986.8	$\frac{5}{2}^-, \frac{7}{2}^-$		
7	<u>1024</u>	(4, 5)	{ 0.0065 if 4 0.0087 if 5	$(\frac{3}{2}^-)$	1024.0	$\frac{5}{2}^-, \frac{7}{2}^+, \frac{9}{2}^-$	1023.7	$(\frac{9}{2}^-)$
					1062.5	$\frac{3}{2}^-, \frac{5}{2}^+$	1062.3	
8	1085	0	0.052	$\frac{1}{2}^-$	1085.4	$\frac{5}{2}^+, \frac{7}{2}^+$	1085.3	
							1086.5	
					1119.8	$\frac{3}{2}^+, \frac{5}{2}^+, \frac{7}{2}^+$		
					1153.3	$(\frac{7}{2}^-)$	1153.1	$(\frac{7}{2}^-)$
					1159.7	$\frac{9}{2}^+, \frac{11}{2}^+, \frac{13}{2}^+$		
					1170	$\frac{3}{2}^-, \frac{5}{2}^-, \frac{7}{2}^-$		
					1180.4	$\frac{3}{2}^+, \frac{5}{2}^+, \frac{7}{2}^-$	1180.4	$(\frac{5}{2}^+, \frac{7}{2}^+)$
9	1201	2	0.018	$\frac{3}{2}^-, \frac{5}{2}^-$	1210.2	$\frac{3}{2}^+, \frac{5}{2}^+, \frac{7}{2}^-$		
10	1284							
11	1299							
12	1419	2	0.009	$\frac{3}{2}^-, \frac{5}{2}^-$				
13	1448	(0)	0.044	$(\frac{1}{2}^-)$				
					1463.1	$\frac{9}{2}^-$		
					1506.1	$\frac{3}{2}^+, \frac{5}{2}^-$		
					1518.8	$\frac{5}{2}^+, \frac{7}{2}^+$	1518.7	$(\frac{5}{2}^+, \frac{7}{2}^+)$

TABLE V. (Continued)

Level No.	E (keV)	Present results			<sup>111</sup> Pd decay <sup>a</sup>		<sup>111</sup> Pd decay <sup>b</sup>	
		L	ε	J <sup>π</sup>	E (keV)	J <sup>π</sup>	E (keV)	J <sup>π</sup>
14	1545	(3)	0.011	$(\frac{5}{2}^+, \frac{7}{2}^+)$	1543	$\frac{9}{2}, \frac{11}{2}, \frac{13}{2}$	1549.4	$\frac{11}{2}^+, \frac{9}{2}^+$
					1549.6	$\frac{9}{2}, \frac{11}{2}$		
15	1602				1622	$\frac{3}{2}, \frac{5}{2}, \frac{7}{2}$		
16	1630	2	0.15	$\frac{3}{2}^-, \frac{5}{2}^-$				
17	1679	2	0.075	$\frac{3}{2}^-, \frac{5}{2}^-$	1705	$\frac{5}{2}^+, \frac{7}{2}^+$	1704.6	$(\frac{5}{2}^+, \frac{7}{2}^+)$
18	1719	0	0.043	$\frac{1}{2}^-$	1706	$\frac{9}{2}, \frac{11}{2}$		
					1748.6	$\frac{9}{2}, \frac{11}{2}, \frac{13}{2}$		
19	1752	2	0.025	$\frac{3}{2}^-, \frac{5}{2}^-$	1781.6	$\frac{9}{2}^-$	1781.6	$\frac{9}{2}^-$
20	1819	2	0.022	$\frac{3}{2}^-, \frac{5}{2}^-$	1821.5	$\frac{9}{2}^-, \frac{11}{2}^-$	1821.3	$\frac{11}{2}^-$
21	1862	2	0.025	$\frac{3}{2}^-, \frac{5}{2}^-$				
					1905.7	$\frac{9}{2}^-, \frac{11}{2}^-$	1905.6	$\frac{11}{2}^-$
22	1934	4	0.012	$\frac{7}{2}^-, \frac{9}{2}^-$			1933.9	
23	1956	(3)	0.025	$(\frac{5}{2}^+, \frac{7}{2}^+)$			1964.6	$\frac{9}{2}^+, \frac{11}{2}^-$
24	1984	3	0.055	$\frac{5}{2}^+, \frac{7}{2}^+$	1987.8	$\frac{9}{2}^-, \frac{13}{2}^-, \frac{11}{2}^-$	1987.9	$\frac{13}{2}^-$
25	2068	3	0.098	$\frac{5}{2}^+, \frac{7}{2}^+$	2069.6	$\frac{9}{2}^-, \frac{11}{2}^-$	2069.5	$\frac{11}{2}^-$
26	2093	3	0.028	$\frac{5}{2}^+, \frac{7}{2}^+$	2087	$\frac{9}{2}^-, \frac{11}{2}^-, \frac{13}{2}^-$		
					2101	$\frac{9}{2}^-, \frac{11}{2}^-$	2101.2	$\frac{11}{2}^-$
27	2125	4	0.005	$\frac{7}{2}^-, \frac{9}{2}^-$				
28	2165	3	0.064	$\frac{5}{2}^+, \frac{7}{2}^+$				
29	2197	(4)	0.012	$(\frac{7}{2}^-, \frac{9}{2}^-)$				
30	2222	(4)	0.029	$(\frac{7}{2}^-, \frac{9}{2}^-)$			2216.7	$\frac{11}{2}^-, \frac{9}{2}^-$
31	2258	5	0.046	$\frac{9}{2}^+, \frac{11}{2}^+$				
32	2282	4	0.043	$\frac{7}{2}^-, \frac{9}{2}^-$				
33	2308	(4)	0.003	$(\frac{7}{2}^-, \frac{9}{2}^-)$				

<sup>a</sup>Reference 34.<sup>b</sup>Reference 35.

The  $L=2$  and  $L=5$  assignments for the states at 2135 and 2283 keV seem quite firm and are in contrast to the  $(1^-)$  and  $(4^+)$  assignments from the  $(p, p')$  data.<sup>33</sup>

E. <sup>111</sup>Ag

The primary sources of information on <sup>111</sup>Ag up to the present time are the results of two investigations<sup>34,35</sup> of the decay of <sup>111</sup>Pd and these results are summarized in Table V. As shown in Fig. 6,  $L=2$  assignments from the  $(t, p)$  data are quite clear for the levels at 290 and 391 keV and from

systematics (as discussed in Sec. V B) the former can be assigned a spin and parity of  $\frac{3}{2}^-$  and the latter  $\frac{5}{2}^-$ . Likewise the two  $L=2$  transitions to the states at 642 and 810 keV are reasonably taken from systematics as the  $\frac{3}{2}^-$  and  $\frac{5}{2}^-$  doublet built on the  $2_2^+$  core state. The states at 846 and 1024 are probably the  $\frac{7}{2}^-$  and  $\frac{9}{2}^-$  states based on the  $4_1^+$  state of the core but the angular distributions shown in Fig. 6 for these states can be described by  $L=5$  about as well as they are by  $L=4$  distorted wave calculations. The  $L=0$  transfers to the states at 1085, 1448, and 1719 keV which have not been seen in other studies, means that a spin

TABLE VI. Optical parameters used in the DWBA analysis. All well depths are in MeV and all distances in fm.

	$V_r$	$r_r$	$a_r$	$\lambda$	$V_I$	$r_I$	$a_I$
Triton	166.7	1.16	0.752		21.4	1.498	0.817
Proton <sup>a</sup>	50.8 <sup>b</sup>	1.25	0.65		14.2 <sup>c</sup>	1.25	0.47
Bound state	d	1.27	0.67	32			

<sup>a</sup>Adjusted slightly for each target mass according to the recipe of Ref. 15.

<sup>b</sup>This value is 3 MeV below the value given in Ref. 15.

<sup>c</sup>Surface form.

<sup>d</sup>Adjusted to fit the binding energy.

and parity of  $\frac{1}{2}^-$  can be assigned to those states. Above 1085 keV few unambiguous correspondences between levels seen in the  $(t, p)$  reaction and those populated in the decay of  $^{111}\text{Pd}$  can be made.

## V. DISCUSSION

### A. Pairing phonon characteristics of $A = 110$ region

The nuclear region examined in the present experiment lies between the closed shell region at  $N \approx 50$  characterized by pairing vibrations and a region of high degeneracy in the tin nuclei characterized by pairing rotations.<sup>36</sup> It also lies very close to a region of shape transitions as seen in the behavior of  $^{102}\text{Mo}$  and, to a lesser extent, in  $^{106}\text{Ru}$ .<sup>37</sup> All of these phenomena would be expected to affect most strongly the behavior of the  $(t, p)$  ground state transitions, the strength to excited  $0^+$  states, and the energy of the lowest  $2^+$  states. Thus an examination of these quantities should lead to the importance of these different concepts in the nuclei examined.

An examination of Tables I through V illustrates the behavior of the ground state strengths. The  $\epsilon$  factors, which correct the cross sections for  $Q$  value and mass differences, indicate near equality for the ground state transitions in Pd and Ag and for the 130 keV state of  $^{105}\text{Rh}$ . This behavior is very characteristic of superconducting nuclei<sup>38</sup> and is in contrast to the region near closed shells; e.g., the zirconium isotopes<sup>39</sup> where factors of 2 in ground state transition strength between isotopes are noted. On the other hand, the ground state enhancement factors are considerably smaller than the values noted in the tin nuclei, indicating less coherency from the neutron orbitals in the nuclei examined here. This is also reinforced by the strength seen to excited  $0^+$  states being 6–8% in the present case and less than 2% for the very superconducting nuclei. Thus the Pd (and Ag) nuclei appear to be somewhat transitional

between a pairing vibration and pairing rotation scheme but much closer to the latter.

The energy systematics of the ground state transitions also yield interesting information. A pairing rotation model implies a parabolic dependence of  $Q$  value or  $B(2n)$  versus neutron number. For the cases observed here between  $N = 62$  and  $N = 64$ , a shift of 803 keV for the Pd nuclei and 835 keV for the Ag nuclei is seen. This shift, which is remarkably equal for the two elements, is again an indicator of pairing rotations. Also of interest is the proton-pairing phonon interaction which produces a shift in binding energy [or  $B(2n)$  as measured here]. The observed shift is 697 keV at  $N = 62$  and 665 keV at  $N = 64$ . This shift, which is a measure of the strength of the vertex for the particle-phonon diagram, again is quite equal for the two cases. This also suggests sufficient degeneracy in neutron orbitals in the pairing phonon such that the addition of two neutrons has little effect on the interaction of the phonon with the valence proton.

### B. Comparisons with weak coupling model

The possible weak coupling relationships for the nuclei studied are shown graphically in Figs. 7 to

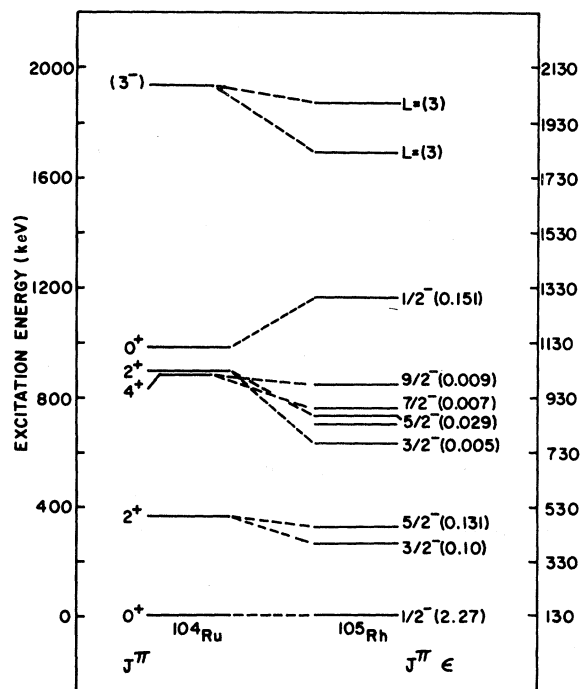


FIG. 7. Candidates for weak coupling states in  $^{105}\text{Rh}$  and the associated core states in  $^{104}\text{Ru}$ . The states in  $^{105}\text{Rh}$  have been shifted by  $-130$  keV in order to align the lowest  $L = 0$  transition with the  $^{104}\text{Ru}$  ground state. See caption for Fig. 8 for further explanation.

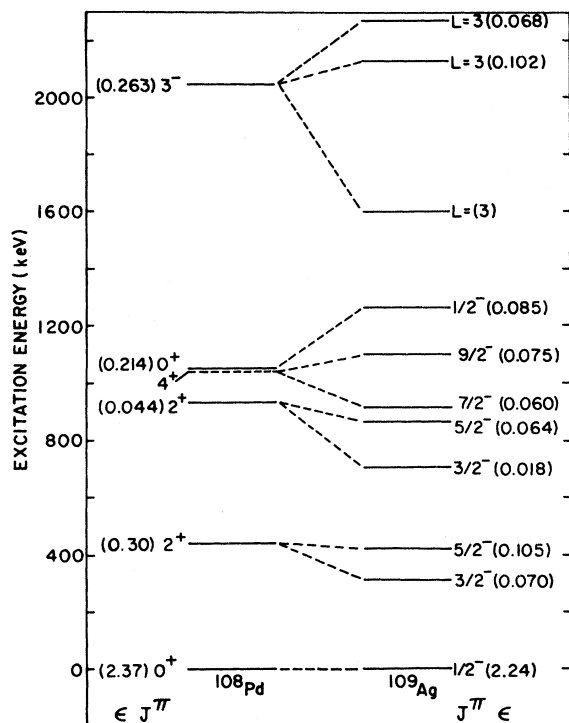


FIG. 8. Candidates for weak coupling states in  $^{109}\text{Ag}$  and the associated core states in  $^{108}\text{Pd}$ . The  $J^\pi$  assignments are made on the basis of the analysis presented in the text and other work, and are relatively well established except for the assignments in parentheses. Only the  $L$  value of the transition is listed for states for which a unique  $J^\pi$  cannot be determined with confidence. Also included in parentheses are the enhancement factors for the transitions in both the even-even and odd- $A$  nuclei.

9 and then numerically in Table VII. The information on the level structure of  $^{104}\text{Ru}$  has been taken from the literature.<sup>40</sup>

The ground state transitions for the  $^{108}\text{Pd}$ - $^{109}\text{Ag}$  and  $^{110}\text{Pd}$ - $^{111}\text{Ag}$  pairs agree well with the predictions of the weak coupling model since the enhancement factors listed in Tables II to V are essentially identical. The quantity  $R'$  in Table VII gives the ratio of summed  $(t, p)$  strength to the core multiplet in the odd- $A$  nucleus,  $\sum \epsilon$  to the  $(t, p)$  strength of the appropriate core transition. In the simple weak coupling model  $R'$  should be equal to 1. As noted above, this is true for the ground states but only 58% of the expected strength is found in  $^{109}\text{Ag}$  and 70% in  $^{111}\text{Ag}$  for the  $2_1^+$  core doublet. The situation changes somewhat for the  $2_2^+$  core doublet where, respectively, 186% and 84% of the expected strengths are found. The  $4_1^+$  state in  $^{108}\text{Pd}$  could not be separated from the strong  $L=0$  transition at 1054 keV. Thus an intensity comparison is available only for  $^{110}\text{Pd}$ -

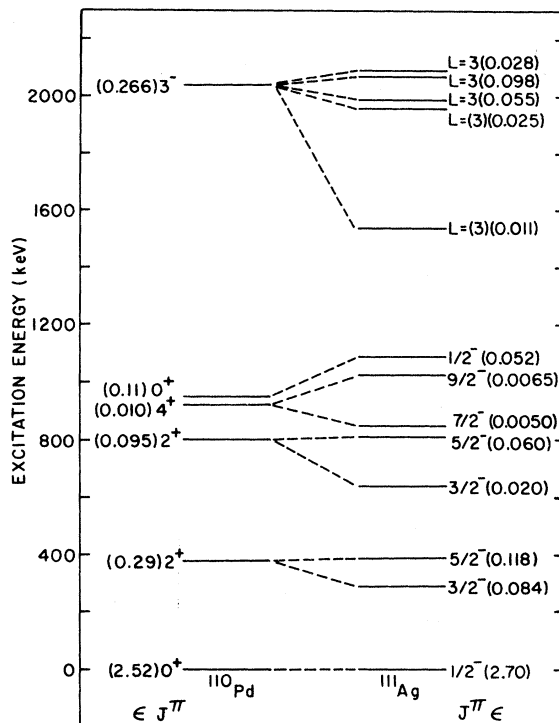


FIG. 9. Candidates for weak coupling states in  $^{111}\text{Ag}$  and the associated states in  $^{110}\text{Pd}$ . See caption for Fig. 8 for further explanation.

$^{111}\text{Ag}$ . In  $^{111}\text{Ag}$ , the angular distributions for the 846 and 1024 keV levels are not definitive, but throughout this analysis these states are assumed to be the  $\frac{7}{2}^-$  and  $\frac{9}{2}^-$  members of the  $4_1^+$  based doublet, respectively. In that context these two levels carry 115% of the expected intensity. The core coupled states based on the  $0^+$  members of the two phonon triplets display a more severe disagreement between the odd- $A$  and even- $A$  enhancement factors than that displayed by the  $2^+$  and  $4^+$  based doublets. In  $^{109}\text{Ag}$ ,  $R'$  is only 0.40 and in  $^{111}\text{Ag}$  it is 0.47. In addition, the higher-lying  $\frac{1}{2}_3^-$  state in  $^{111}\text{Ag}$  contains 65% of the strength of the corresponding state in  $^{110}\text{Pd}$ .

Another property that can be tested against the weak coupling model is the position of the centroid of the doublet relative to the parent state in the even-even nucleus. In the simplest form of the model there should be no shift. The data, however, as displayed in Table VII show shifts for all cases. The quantity  $\Delta'$ , which indicates the energy of the multiplet centroid minus the energy of the core state, is -60, -61, and -25 keV for the  $2_1^+$  core doublets in  $^{105}\text{Rh}$ ,  $^{109}\text{Ag}$ , and  $^{111}\text{Ag}$ , respectively. In this case and in the following paragraph, the excitation energies of the centroids in  $^{105}\text{Rh}$  are calculated relative to the  $\frac{1}{2}^-$  state at

TABLE VII. Weak coupling comparisons for the five nuclei studied. All of the listed quantities are defined in the text.

Residual nucleus	$E$ (keV)	Multiplet centroid energy (keV)	$E_{\text{core}}$ (keV)	$\Delta$ (keV)	$\Delta'$ (keV)	$R$	$R_{\text{th}}$	$\sum \epsilon$	$R'$	$\Delta_{\text{th}}$ (keV)
$^{105}\text{Rh}$	0.0	0.0	$0_1^+$ 0.0	...	...	...	...	2.27	...	...
	392 456	428	$2_1^+$ 358	64	-60 <sup>a</sup>	0.76	0.66	0.231	...	70
	762 868	852	$2_2^+$ 893	106	-171 <sup>a</sup>	0.17	0.66	0.034	...	99
	1297	1297	$0_2^+$ 987	...	+180 <sup>a</sup>	...	...	0.151	...	...
	896 976	941	$4_1^+$ 888	80	-77 <sup>a</sup>	0.78	0.80	0.016	...	104
	$^{109}\text{Ag}$	0.0	0.0	$0_1^+$ 0.0	...	...	...	...	2.24	0.95
311 415		373	$2_1^+$ 434	104	-61	0.67	0.66	0.175	0.58	112
702 863		828	$2_2^+$ 931	161	-103	0.28	0.66	0.082	1.86	167
912 1091		1012	$4_1^+$ 1048	179	-36	0.80	0.80	0.135	...	184
1260		1260	$0_2^+$ 1054	...	+206	...	...	0.085	0.40	...
$^{111}\text{Ag}$		0.0	0.0	$0_1^+$ 0.0	...	0.0	...	...	2.70	1.07
	290 391	349	$2_1^+$ 374	101	-25	0.71	0.66	0.202	0.70	108
	642 810	768	$2_2^+$ 814	168	-46	0.33	0.66	0.080	0.84	160
	846 1024	947	$4_1^+$ 921	178	+26	0.77	0.80	0.0115	1.15	178
	1085	1085	$0_2^+$ 946	...	+139	...	...	0.052	0.47	...
	1448	1448	$0_3^+$ 1175	...	+273	...	...	0.044	0.65	...

<sup>a</sup>Relative to 130 keV state.

130 keV. The centroids of the higher-lying  $2_2^+$  core doublets are shifted downwards by somewhat larger amounts. In contrast, the singlet  $\frac{1}{2}^-$  levels based on the  $0_2^+$  and  $0_3^+$  core states are all much more severely shifted. These states seen are shifted upwards by amounts that range from 139 to 273 keV. Because the higher-lying  $\frac{1}{2}^-$  levels in all three odd-A nuclei deviate substantially both in intensity and excitation energy compared to the corresponding  $0^+$  states in the even-even cores, the weak coupling association of the appropriate pairs seems quite tenuous. The  $4_1^+$  core doublets are displaced by smaller amounts of -77, -36, and +26 keV for  $^{105}\text{Rh}$ ,  $^{109}\text{Ag}$ , and  $^{111}\text{Ag}$ . A feature of the latter doublets is that while the deviations are not as large as those encountered for the  $2_2^+$  and  $0_2^+$  based states, they no longer exhibit a systematic behavior since the  $^{109}\text{Ag}$  and  $^{111}\text{Ag}$  shifts

are in opposite directions.

The statistical weighting factor should give the ratio  $R$  of the enhancement factors of the members of the various core multiplets. For example, the ratio of the enhancement factors for the  $\frac{3}{2}^-$  and  $\frac{5}{2}^-$  states based on a  $2^+$  core state should be  $2J_1 + 1 / 2J_2 + 1$  or 0.67. In Table VII the columns marked  $R$  and  $R_{\text{th}}$  indicate the experimental and theoretical values for this ratio. For the  $2_1^+$  based core doublet the experimental ratios for the three nuclei are remarkably close to the theoretical value. Since in all three nuclei at least one member of the doublet has a spin and parity assignment firmly established by other studies, the  $2J + 1$  rule is unambiguously verified for these cases. The  $2_2^+$  based doublets show rather large deviations from the theoretical value with ratios of 0.17, 0.28, and 0.33 for  $^{105}\text{Rh}$ ,  $^{109}\text{Ag}$ , and  $^{111}\text{Ag}$ , respectively,

where the value quoted for  $^{105}\text{Rh}$  is based on the 762 and 868 keV levels. The  $4_1^+$  based doublets on the other hand are reasonably close to the theoretical value of 0.80 with values of 0.78, 0.80, and 0.77 for  $^{105}\text{Rh}$ ,  $^{109}\text{Ag}$ , and  $^{111}\text{Ag}$ . All of these ratios are consistent with the general observation that the lower spin member of the doublet lies lowest in excitation energy. Where other studies have provided spin and parity assignments they, too, are consistent with this observation.

### C. Deviations from weak coupling predictions

There are two principle reasons for deviations from a simple weak coupling model; mixing between members of different multiplets and mixing between multiplet members and states of the same spin and parity but of different parentage. The first problem will be most important if the multiplet is quite spread in energy or if two core-phonons of the same spin and parity are located at nearly the same excitation energy. The second mixing situation occurs if states belonging to other elementary excitations, e.g., single-particle or particle-hole states, lie in the same region of excitation. This mixing will be especially strong if there is a near degeneracy in energy and for cases where the spin-coupling coefficients are large. Such couplings have been considered theoretically for a more general particle-vibration case.<sup>7</sup>

There is the additional problem of the choice of basic phonon states; i.e., does a  $p_{1/2}$  proton coupled to Pd or a  $p_{1/2}$  hole coupled to Cd offer the best description of the Ag isotopes. In either situation the assumption is that the average potential felt by the neutrons, especially the neutrons near the Fermi level, is not changed by the addition of a particle (hole). We know, of course, that this is not strictly true, and thus the "true" core state is probably best represented by a mixture of states from Pd and Cd. However, at least one feature of weak coupling is likely to remain in spite of such mixing. Let us take the doublets based on the  $2_1^+$  states as examples.

As mentioned previously, the  $2_1^+$  based doublets in  $^{109}\text{Ag}$  and  $^{111}\text{Ag}$  (as well as  $^{105}\text{Rh}$ ) follow the  $(2J+1)$  rule but retain only 70% of the intensity of the  $2_1^+$  states in  $^{108,110}\text{Pd}$ . On the other hand,  $(t, p)$  studies on the odd- $A$  nuclei  $^{209}\text{Pb}$ <sup>41</sup> and  $^{209}\text{Bi}$ <sup>42</sup> show that the  $(2J+1)$  rule is not followed, but that the full intensity of the core is present in the odd- $A$  multiplet. Thus the lowest  $L=2$  phonons in pairing rotational nuclei appear to retain their collective character when the valence nucleon is added due to the high neutron degeneracy present. In contrast, the  $2_1^+$  states in the lead region are dominated by a particular single-particle orbital

and hence, they do not have the stability of the more collective phonons in the Pd nuclei. Because the  $(2J+1)$  rule represents a purely statistical division of the transition intensity depending only on the collective properties of the core phonon, we expect that this rule would be followed by all weak coupling doublets based on highly collective states such as the low-lying states in pairing rotational nuclei. On the other hand, mixing of the Pd-Cd core states could lead to a different transition intensity compared to the case where the  $2_1^+$  phonons in the Pd nuclei represented the true core states. However, whether the true core state is best described by the  $2_1^+$  phonon in Pd, in Cd, or as a mixture of the two, we would still expect the  $(2J+1)$  rule to hold, with only possibly a small change in the total transition intensity. This is exactly the behavior seen for the core coupled  $\frac{3}{2}^-$  and  $\frac{5}{2}^-$  states observed.

Mixing of the core coupled states with single-particle states of the appropriate  $J^\pi$  also occurs. For example, the  $\frac{3}{2}^-$  members of the core coupled doublets based on the  $2_1^+$  and  $2_2^+$  states are comparably excited<sup>43</sup> in the  $(^3\text{He}, d)$  reactions on  $^{104,106,110}\text{Pd}$ . While the  $\frac{3}{2}^-$  311 keV state in  $^{109}\text{Ag}$  is also excited<sup>31</sup> in the  $(^3\text{He}, d)$  reaction, the  $\frac{3}{2}^-$  702 keV state appears to be obscured by the strong  $l=0$  transition to the  $\frac{1}{2}^+$  state at 706 keV. In the  $^{104}\text{Ru}(^3\text{He}, d)^{105}\text{Rh}$  reaction<sup>21</sup> the 392 keV state was excited but the 762 keV state was assigned  $l=2$ , which is inconsistent with the  $J^\pi = \frac{3}{2}^-$  assigned in this work. The authors point out, however, that the rather structureless nature of the  $(^3\text{He}, d)$  angular distributions made assignments of  $l$  values ambiguous. The angular distribution which they observe for the 762 keV state appears to be consistent with  $l=1$  and, if this is so, all of the  $\frac{3}{2}^-$  members of the core coupled doublets based on the  $2_1^+$  and  $2_2^+$  states are mixed with the  $2p_{3/2}$  single-particle orbital. In the four cases where the mixing ratio can be determined, the mixing is severe in that about equal amounts of the  $2p_{3/2}$  single-particle strength appear in each level. However, since only about 10% of the total single-particle strength is involved, the weak coupling character of the state is not strongly altered. There is some evidence from single-particle transfer reactions<sup>31,43,44</sup> for mixing of the  $\frac{5}{2}^-$  core excited states with the  $1f_{5/2}$  single-particle level. In the isolated cases where these  $\frac{5}{2}^-$  states have been seen in  $(^3\text{He}, d)$  work,<sup>31,43</sup> they are very weakly excited with noncharacteristic angular distributions. However, significant amounts of  $1f_{5/2}$  strength are observed in the low-lying  $\frac{5}{2}^-$  states in  $^{109}\text{Ag}$  and  $^{111}\text{Ag}$  in studies of the  $\text{Cd}(d, ^3\text{He})\text{Ag}$  reactions.<sup>44</sup> Wave functions<sup>3</sup> for these levels obtained by fitting  $B(E2)$  and  $(p, t)$  data indicate a substantial ampli-

tude for the  $1f_{5/2}$  single-particle orbital while other calculations<sup>45</sup> disagree. Calculations<sup>46</sup> which restrict the odd proton to the  $1g_{9/2}$ ,  $2p_{1/2}$ , and  $2p_{3/2}$  levels have also been made and will be discussed later.

Mixing with states of single-particle character could possibly account for the deviation from the  $(2J+1)$  rule for the  $2_2^+$  based doublets. It is not immediately clear why the  $2_1^+$  based doublet is less severely affected. However, this lowest-lying phonon would presumably contain the greatest coherency due to the multipole pairing force. In addition, both members of the  $2_2^+$  based doublet are mixed with single-particle levels (about 10% of the total single-particle strength is involved) while only the  $\frac{3}{2}^-$  member of the  $2_1^+$  doublet is mixed.

No traces of the  $\frac{7}{2}^-$  and  $\frac{9}{2}^-$  members of the  $4_1^+$  based doublets were found in any of the ( $^3\text{He}, d$ ) or ( $d, ^3\text{He}$ ) work. The  $\frac{9}{2}^-$  member would certainly be excited in the former and the  $\frac{7}{2}^-$  member in the latter if any substantial mixing with the  $1h_{9/2}$  and  $1f_{7/2}$  single-particle orbitals were present. Lack of such mixing is probably the reason that the  $4_1^+$  based doublets, in addition to the lowest  $L=0$  transitions, represent the best examples of weak coupled states seen in this work.

One might at first anticipate that doublets based on the very collective  $3^-$  states would exhibit good weak coupling behavior. However, the  $3^-$  states in Pd occur at  $E_x \approx 2$  MeV and it is just this region of excitation where strong fragments of the  $1g_{7/2}$  and  $2d_{5/2}$  single-particle orbitals are found in the odd-Ag isotopes.<sup>31,43</sup> Thus, it would not be at all surprising if these states were to mix with the  $\frac{5}{2}^+$  and  $\frac{7}{2}^+$  core excited states leading to several  $L=3$  transitions in the odd-A nuclei. This is borne out in  $^{111}\text{Ag}$  where at least three and perhaps as many as five  $L=3$  transitions are seen. If all five transitions are indeed  $L=3$ , then all of the strength of the  $3^-$  state at 2038 keV in  $^{110}\text{Pd}$  is found in  $^{111}\text{Ag}$ . In the ( $^3\text{He}, d$ ) work it appears that two of these levels, the 1984 and 2093 keV states, are excited. A level at 1986 keV is excited with an  $l=2$  angular distribution ( $j^\pi = \frac{3}{2}^+$  or  $\frac{5}{2}^+$ ) while a level at 2093 keV is excited with an  $l=4$  angular distribution ( $j^\pi = \frac{7}{2}^+$  or  $\frac{9}{2}^+$ ). The latter level is almost undoubtedly  $\frac{7}{2}^+$  since essentially all of the available  $1g_{9/2}$  strength is exhausted by the 130 keV level. In  $^{109}\text{Ag}$  there are two definite and one possible  $L=3$  transitions, but about 30% of the  $3^-$  strength in  $^{109}\text{Pd}$  is still missing. Thus the  $L=3$  based doublets in both Ag nuclei studied are very strongly perturbed by mixing with the  $1g_{7/2}$  and  $2d_{5/2}$  single-particle orbitals and do not represent good examples of weakly coupled states.

The next class of mixing which may be con-

sidered occurs when two core states in the same nucleus mix, e.g., the  $0_1^+$  and  $0_2^+$  states in  $^{108}\text{Pd}$  may each be present in the wave functions for both the  $\frac{1}{2}_1^-$  and  $\frac{1}{2}_2^-$  states in  $^{109}\text{Ag}$ . If the weak coupling picture of the 1260 keV state in  $^{109}\text{Ag}$  as a  $2p_{1/2}$  proton coupled to the 1054 keV state in  $^{108}\text{Pd}$  were strictly correct and the ground and 1054 keV states in  $^{108}\text{Pd}$  were not mixed, then the 1260 keV state in  $^{109}\text{Ag}$  would not be observed in the ( $^3\text{He}, d$ ) reaction. However, in Ref. 31 we see that this level is excited with an  $l=1$  transition and an intensity of about 3% of that of the ground state. Assuming a one-step reaction mechanism, there then must be some mixing of the core states (i.e.,  $^{108}\text{Pd}$  ground and 1054 keV states) for these  $\frac{1}{2}^-$  states. The mixing of the  $0_1^+$  and  $0_2^+$  core states appears small, and this observation is consistent with the wave functions given in Refs. 3 and 46. The  $2_1^+$  and  $2_2^+$  states, however, are only about 500 keV apart and significant mixing is predicted in Ref. 46. It seems likely that such mixing would also occur for particle-phonon states in  $^{111}\text{Ag}$  based on the  $0_2^+$  and  $0_3^+$  states at 946 and 1175 keV in  $^{110}\text{Pd}$ . A more complex form of this type of mixing occurs when higher-order diagrams which couple several core phonons and single-particle orbitals are included, e.g., one may find a  $|2_2^+ \otimes 2p_{3/2}; \frac{3}{2}^- \rangle$  component in the nominally  $|2_1^+ \otimes 2p_{1/2}; \frac{3}{2}^- \rangle$  state. Such mixing is predicted in Ref. 46 although it is difficult to make detailed comparisons of those calculations to the present results because the two nucleon overlaps are not presented.

The picture which emerges from the silver nuclei studied, and to a lesser extent from the  $^{105}\text{Rh}$  nucleus, is that a weak coupling identification may be made for the major parentage of low-lying states in odd-A nuclei in this mass region. Changes in the character of the core states in silver compared to palladium do not appear to result in qualitative differences from the predictions of the weak coupling model although quantitative differences are noted. Variations in the centroid excitation energies and total transition intensities for some doublets occur as well as a breakdown of the  $(2J+1)$  rule for the  $2_2^+$  based doublets, but the particle-phonon states still appear as doublets based on the core state. A possible exception is the  $2_2^+$  based doublet in  $^{105}\text{Rh}$  where a third transition is seen in the region of the anticipated doublet. However, the  $L$  value is not established and the intensity is about an order of magnitude smaller than that of the 762 and 868 keV states. On the other hand, the  $0_1^+$  and  $4_1^+$  based states in the odd-A nuclei follow the weak coupling predictions quite nicely. Other expected  $\frac{1}{2}^-$  states appear as singlets with changes in the total transition strengths and excitation energies

noted. These results differ from those obtained in studies<sup>47,48</sup> of the  $^{89}\text{Y}(t,p)^{91}\text{Y}$  and  $^{89}\text{Y}(p,t)^{87}\text{Y}$  reactions. In those studies more severe deviations from the simple predictions of the weak coupling model were noted since, in general, the multiplet centroids and strengths deviate more from the expected values (although a different choice of the core could improve this). In addition, the anticipated doublets in  $^{87}\text{Y}$  actually appear as quartets, indicating a more severe mixing with other modes of excitation. A study<sup>49</sup> of  $^{91}\text{Zr}$  using the  $(d,p)$ ,  $(p,d)$ , and  $(p,p')$  reactions led to the same conclusion for that nucleus. Why then does the weak coupling approach work reasonably well in the Rh-Ag region? The explanation probably lies in the coherence properties of the core states. These states must be collective in character and maintain this character despite the addition of the valence particle. The lowest  $L=0$  transitions in  $^{105}\text{Rh}$ ,  $^{109,111}\text{Ag}$ , and  $^{108,110}\text{Pd}$  indicate that these are superconducting nuclei. Essentially no change in the enhancements of the lowest  $L=0$  transitions are seen even though  $^{105}\text{Rh}$  and  $^{111}\text{Ag}$  differ by two protons and four neutrons. The highly correlated character of the ground states in superconducting nuclei appears to make them extremely stable and insensitive to small changes in the average potential. In addition, the  $2_1^+$  and  $4_1^+$  states appear also to retain this stability. Of course, this situation is the one which most nearly fulfills the basic assumption of the weak coupling model. Conversely, the  $^{87,91}\text{Y}$  and  $^{91}\text{Zr}$  nuclei are near the shell closure at  $N=50$  and do not possess the pairing collective character of the core states in the Pd region. This also means that our data argue against any strong shell closure at  $N=64$ , although the  $0_2^+$  states in  $^{108,110}\text{Pd}$  are populated rather more strongly than one might anticipate in superconducting nuclei. In this sense they resemble the  $^{112}\text{Sn}(t,p)^{114}\text{Sn}$  results<sup>50</sup> rather than those<sup>38,50,51</sup> for Sn targets with  $A \geq 116$ . Thus the rather strong population of the  $0^+$  member of the two phonon triplet in the even nuclei is a consistent feature of  $(t,p)$  studies on nuclei with  $60 \leq N \leq 64$ , and as mentioned previously, our data lend support to the assumption that the nuclei in this mass region are of a transitional character, though more closely evidencing the properties of pairing rotational nuclei than pairing vibrational nuclei.

#### D. Details of the particle-core interaction

The object of the weak coupling model is to relate the properties of the core coupled states to the properties of the core states and the valence particle in a simple fashion. Empirically, we see

from Table VII that the doublet splittings in  $^{109}\text{Ag}$  and  $^{111}\text{Ag}$  for the  $2_1^+$ ,  $2_2^+$ , and  $4_1^+$  based doublets can be reproduced (to within 10%) by the formula

$$\Delta_{\text{th}} = kE_x^{1/2} \quad (1)$$

where  $\Delta_{\text{th}}$  is the doublet splitting,  $k$  is a constant with the value of 5.8, and  $E_x$  is the excitation energy of the centroid of the doublet (the excitation energy of the core state might be substituted for  $E_x$  with only a slight change in the results). That such a simplistic approach can reproduce the splitting of six doublets based on phonons of differing multipolarity in two different nuclei is quite remarkable and is difficult to understand. This is especially true in view of the fact that the collectivity of the core states, for example the deformation parameter, is different for the first and second phonons. In  $^{105}\text{Rh}$  we may again reproduce the doublet splittings (see Table VII), but a new value of 3.4 for  $k$  is necessary. Unless this agreement is strictly fortuitous, a formulation such as given in (1) suggests that the particle-core interaction cannot be proportional to  $(\vec{J}_c \cdot \vec{J}_p)$ , the simplest scalar interaction which depends on  $\vec{J}_c$  (the spin of the core state) and  $\vec{J}_p$  (the spin of the valence particle), since  $\vec{J}_c \cdot \vec{J}_p$  is not constant for  $J_c=2$  and  $J_c=4$ . In this context it might be interesting to observe the  $(t,p)$  reaction for odd-proton nuclei in this region which have  $J_p \neq \frac{1}{2}$ . However, a comparison of that data with the present experiment must be undertaken with caution since, when  $J_p \neq \frac{1}{2}$ , tensor operators of rank greater than one may contribute to the interaction<sup>2</sup> which splits the members of a given multiplet.

It is a more difficult task to evaluate the centroid shifts of the core coupled states relative to the core states. This is illustrated by the fact that while the  $4_1^+$  based doublets in  $^{109}\text{Ag}$  and  $^{111}\text{Ag}$  both shift about 30 keV from the corresponding core states, they shift in opposite directions. In addition, there appears to be no simple formulation which reproduces even the magnitudes of the shifts of the centroids of the doublets relative to the core states. Thus, it seems that while the doublet splittings follow a simple empirical regularity, the positions of the energy centroids do not.

#### E. Comparisons to predictions of the Alaga model

Paar<sup>46</sup> has made calculations involving the coupling of three particles or holes to quadrupole vibrations. For the odd- $A$  silver isotopes he took a three proton-hole cluster moving in the  $g_{9/2}$ ,  $p_{1/2}$ , and  $p_{3/2}$  shell model orbitals coupled to a quadrupole vibrational field with vibrator states of up to three phonons. Only a few of the results

of his calculations can be directly compared to the results of the  $(t, p)$  studies. He predicts the energies of the levels of  $^{107}\text{Ag}$  and  $^{109}\text{Ag}$  and in fact has the correct ordering for the first six excited states. In general he predicts these levels to lie somewhat higher in energy than is given by experiment. For example, the lowest  $\frac{9}{2}^-$  and  $\frac{7}{2}^-$  levels in  $^{109}\text{Ag}$  are predicted to be at about 1330 and 1030 keV while in reality they are 1091 and 912 keV. The lowest  $\frac{1}{2}^-$  excited state in  $^{109}\text{Ag}$  is predicted to be around 2000 keV while it is actually at 1260 keV, which in turn is considerably above the position of the  $0^+$  core state at 1054 keV. Above this point the comparison of theory and experiment becomes rather inconclusive. It is apparent from Paar's calculations, however, that while the major part of the wave functions for the low-lying states of  $^{109}\text{Ag}$  have the simple weak coupling components, other components play an important role.

For example, if the two  $g_{9/2}$  hole states are recoupled to spins of 2 and 4, then various 0, 1, and 2 phonon states can be coupled using either a  $p_{1/2}$  or  $p_{3/2}$  proton state to form from six to eight important components of the wave function.

#### ACKNOWLEDGMENTS

The authors would like to acknowledge the assistance of a number of individuals at Los Alamos Scientific Laboratory: Ms. J. Gursky who prepared the  $^{103}\text{Rh}$  target used in this work, Mr. S. Orbesen and the crew of the Los Alamos tandem van de Graaff for smooth operation of the facilities, and Dr. J. Sunier and Dr. R. Poore for their assistance in using the computer and data handling routines. Finally, the authors would like to thank Dr. J. A. Grau for making available data on  $^{105}\text{Rh}$  prior to publication.

\*Work supported by the U.S. Energy Research and Development Administration and by the National Science Foundation.

†Present address: Nuclear Physics Laboratory, University of Pittsburgh, Pittsburgh, Pennsylvania 15260.

<sup>1</sup>R. D. Lawson and J. L. Uretsky, *Phys. Rev.* **108**, 1300 (1957).

<sup>2</sup>A. de Shalit, *Phys. Rev.* **122**, 1530 (1961).

<sup>3</sup>A. W. Kuhfeld and N. M. Hintz, *Nucl. Phys.* **A247**, 152 (1975).

<sup>4</sup>R. M. Del Vecchio, I. C. Oelrich, and R. A. Naumann, *Phys. Rev. C* **12**, 845 (1975).

<sup>5</sup>R. M. Del Vecchio, R. A. Naumann, J. R. Duray, H. Hübel, and W. W. Daehnick, *Phys. Rev. C* **12**, 69 (1975).

<sup>6</sup>B. R. Mottelson, *J. Phys. Soc. Jpn. Suppl.* **24**, 87 (1968).

<sup>7</sup>D. R. Bes and R. A. Broglia, *Phys. Rev. C* **3**, 2349 (1971).

<sup>8</sup>A. Bohr and B. Mottelson, *Annu. Rev. Nucl. Sci.* **23**, 363 (1973).

<sup>9</sup>E. R. Flynn, S. Orbesen, J. D. Sherman, J. W. Sunier, and R. Woods, *Nucl. Instrum. Methods* **128**, 35 (1975).

<sup>10</sup>S. D. Orbesen, J. D. Sherman, and E. R. Flynn, Los Alamos Report No. LA-6271-MS, 1976 (unpublished).

<sup>11</sup>Program AUTOFIT, J. R. Comfort, ANL Report No. PHY-1970B (unpublished).

<sup>12</sup>J. F. Mateja, J. A. Bieszk, J. T. Meek, J. D. Goss, A. A. Rollefson, P. L. Jolivet, and C. P. Browne, *Phys. Rev. C* **13**, 2209 (1976).

<sup>13</sup>P. D. Kunz (private communication).

<sup>14</sup>B. F. Bayman and A. Kallio, *Phys. Rev.* **156**, 1121 (1967).

<sup>15</sup>F. G. Perey, *Phys. Rev.* **131**, 745 (1963).

<sup>16</sup>E. R. Flynn, D. D. Armstrong, J. G. Beery, and A. G. Blair, *Phys. Rev.* **182**, 1113 (1969).

<sup>17</sup>F. E. Bertrand, *Nucl. Data Sheets* **11**, 449 (1974).

<sup>18</sup>N. K. Aras and W. B. Walters, *Phys. Rev. C* **11**, 927 (1975).

<sup>19</sup>J. A. Grau, L. E. Samuelson, P. C. Simms, S. I. Popik,

and F. A. Rickey, *Bull. Am. Phys. Soc.* **21**, 95 (1976).

<sup>20</sup>E. Schneider, G. Mathews, S. Jackson, P. Gallagher, and W. B. Walters, *Phys. Rev. C* **13**, 1624 (1976).

<sup>21</sup>D. L. Dittmer and W. W. Daehnick, *Phys. Rev. C* **2**, 238 (1970).

<sup>22</sup>F. E. Bertrand, *Nucl. Data* **B7**, 33 (1972).

<sup>23</sup>K. Okano, Y. Kawase, S. Uehara, and T. Hayashi, *Nucl. Phys.* **A164**, 545 (1971).

<sup>24</sup>N. D. Johnson, J. H. Hamilton, A. F. Kluk, and N. R. Johnson, *Z. Phys.* **243**, 395 (1971).

<sup>25</sup>J. H. Hamilton, S. M. Brahmavar, J. B. Gupta, R. W. Lide, and P. H. Stelson, *Nucl. Phys.* **A172**, 139 (1971).

<sup>26</sup>M. Behar, K. S. Krane, R. M. Steffen, and M. E. Bunker, *Nucl. Phys.* **A201**, 126 (1973).

<sup>27</sup>L. I. Govor, A. M. Demidov, I. B. Shukalov, M. R. Ahmed, Kh. I. Shakarchi, S. Al-Najjar, M. A. Al-Amili, and N. Al-Assafi, *Nucl. Phys.* **A245**, 13 (1975).

<sup>28</sup>M. Koike, T. Suehiro, K. Pingel, K. Komura, I. Nonaka, T. Wada, T. Fujisawa, H. Kamitsubo, and T. Nojiri, *Nucl. Phys.* **A248**, 237 (1975).

<sup>29</sup>F. E. Bertrand, *Nucl. Data* **B6**, 1 (1971).

<sup>30</sup>J. L. C. Ford, Jr., R. L. Robinson, P. H. Stelson, T. Tamura, and Cheuk-Yin Wong, *Nucl. Phys.* **A142**, 525 (1970).

<sup>31</sup>R. L. Auble, F. E. Bertrand, Y. A. Ellis, and D. J. Horen, *Phys. Rev. C* **8**, 2308 (1973).

<sup>32</sup>F. E. Bertrand and S. Raman, *Nucl. Data* **B5**, 487 (1971).

<sup>33</sup>R. L. Robinson, J. L. C. Ford, Jr., P. H. Stelson, T. Tamura, and C. Y. Wong, *Phys. Rev.* **187**, 1609 (1969).

<sup>34</sup>G. Berzins, M. E. Bunker, and J. W. Starner, *Nucl. Phys.* **A126**, 273 (1969).

<sup>35</sup>W. C. Schick, Jr., and W. L. Talbert, Jr., *Nucl. Phys.* **A128**, 353 (1969).

<sup>36</sup>A. Bohr, in *Proceedings of the International Symposium on Nuclear Structure, Dubna, 1968* (IAEA, Vienna, Austria, 1969), p. 169.

<sup>37</sup>R. F. Casten, E. R. Flynn, O. Hansen, and T. J. Mul-

- ligan, Nucl. Phys. A184, 357 (1972).
- <sup>38</sup>E. R. Flynn, J. G. Beery, and A. G. Blair, Nucl. Phys. A154, 225 (1970).
- <sup>39</sup>E. R. Flynn, J. G. Beery, and A. G. Blair, Nucl. Phys. A218, 285 (1974).
- <sup>40</sup>L. E. Samuelson, W. H. Kelly, R. L. Auble, and W. C. McHarris, Nucl. Data Sheets 18, 125 (1976).
- <sup>41</sup>E. R. Flynn, G. Igo, P. D. Barnes, D. Kovar, D. Bes, and R. Broglia, Phys. Rev. C 3, 2371 (1971).
- <sup>42</sup>E. R. Flynn, J. D. Sherman, J. W. Sunier, and D. G. Burke, Nucl. Phys. A263, 365 (1976).
- <sup>43</sup>R. E. Anderson and J. J. Kraushaar, Nucl. Phys. A241, 189 (1975); R. E. Anderson, R. L. Bunting, J. D. Burch, S. R. Chinn, J. J. Kraushaar, R. J. Peterson, D. E. Prull, B. W. Ridley, and R. A. Ristinen, *ibid.* A242, 75 (1975); R. E. Anderson, J. J. Kraushaar, R. A. Emigh, P. A. Batay-Csorba, and H. P. Blok (unpublished).
- <sup>44</sup>S. Y. vander Werf, B. Fryszczyn, L. W. Put, and R. H. Siemssen, Kernfysisch Versneller Instituut, Groningen, The Netherlands (unpublished).
- <sup>45</sup>S. C. Gujrathi and B. P. Pathak, Lett. Nuovo Cimento 1, 887 (1971).
- <sup>46</sup>V. Paar, Nucl. Phys. A211, 29 (1973).
- <sup>47</sup>B. M. Preedom, E. R. Flynn, and N. Stein, Phys. Rev. C 11, 1691 (1975).
- <sup>48</sup>I. C. Oelrich, K. Krien, R. M. Del Vecchio, and R. A. Naumann (unpublished).
- <sup>49</sup>H. P. Blok, L. Hulstman, E. J. Kaptein, and J. Blok (private communication).
- <sup>50</sup>J. H. Bjerregaard, O. Hansen, O. Nathan, R. Chapman and S. Hinds, Nucl. Phys. A131, 481 (1969).
- <sup>51</sup>J. H. Bjerregaard, O. Hansen, O. Nathan, L. Vistinsen, R. Chapman, and S. Hinds, Nucl. Phys. A110, 1 (1968).